Am J Cancer Res 2022;12(5):2397-2418
www.ajcr.us /ISSN:2156-6976/ajcr0138865

Original Article

Bioinformatics analysis of potential Key lncRNA-miRNA-mRNA molecules as prognostic markers and important ceRNA axes in gastric cancer

Siqi Tang[1,2*], Keyong Liao[1,2*], Yongpeng Shi[1,2*], Tingting Tang[1], Beibei Cui[1], Zunnan Huang[1,3]

[1]Key Laboratory of Big Data Mining and Precision Drug Design of Guangdong Medical University, Key Laboratory for Research and Development of Natural Drugs of Guangdong Province, School of Pharmacy, Guangdong Medical University, Dongguan 523808, Guangdong, China; [2]The Second School of Clinical Medicine, Guangdong Medical University, Dongguan 523808, Guangdong, China; [3]Marine Medical Research Institute of Guangdong Zhanjiang, Zhanjiang 524023, Guangdong China. [*]Equal contributors.

Received September 4, 2021; Accepted March 11, 2022; Epub May 15, 2022; Published May 30, 2022

Abstract: Gastric cancer (GC), the fifth most common malignancy worldwide, has an extremely poor prognosis at the advanced stage or the early stage if inadequately treated. Long noncoding RNAs (lncRNAs), microRNAs (miRNAs) and mRNAs all function as competing endogenous RNAs (ceRNAs) that target and regulate each other. Changes in their expression and their regulatory bioprocesses play important roles in GC. However, the roles of key RNAs and their regulatory networks remain unclear. In this study, RNA profiles were extracted from The Cancer Genome Atlas database, and R language was used to discover the differentially expressed (DE) lncRNAs, miRNAs and mRNAs in GC. Then, the DERNAs were paired by miRcode, miRDB, TargetScan and DIANA, and the ceRNA network was further constructed and visualized using Cytoscape. Moreover, a functional enrichment analysis was performed using Metascape. Afterward, the "survival" package was employed to identify candidate prognostic targets (DERNA-os) in the ceRNA network. Ultimately, the ceRNA network was analyzed to identify crucial lncRNA/miRNA/mRNA axes. Based on 374 gastric adenocarcinoma and gastric adenoma samples, 283 DEceRNAs (69 lncRNAs, 10 miRNAs, and 204 mRNAs) were identified. The 204 mRNAs were significantly enriched in some interesting functional clusters, such as the trans-synaptic signaling cluster and the protein digestion and absorption cluster. The ceRNA network consisted of 43 ceRNAs (13 lncRNAs, 2 miRNAs, and 28 mRNAs) that were related to prognosis. Among them, 2 lncRNAs (LNC00469 and AC010145.1) and 1 mRNA (PRRT4) were potential new biomarkers. In addition, according to the lncRNA/miRNA/mRNA regulatory relationships among the 43 ceRNAs, we identified four axes that might play important roles in the progression of GC and investigated the potential mechanism of the most promising axis (POU6F2-AS2/hsa-mir-137/OPCML) in promoting the proliferation and invasiveness of GC.

Keywords: Gastric cancer, miRNA, lncRNA, mRNA, ceRNA

Introduction

Gastric cancer (GC) is the fifth most common malignancy worldwide [1]. Approximately 1,089,103 people were diagnosed with GC in 2020 [1]. The age-standardized incidence rate of stomach cancer in men is 2-fold higher than that in women [1]. GC ranks fourth in cancer-related mortality worldwide, and approximately 768,793 people died of this disease in 2020 [1]. In China, the number of males and females who died from GC is approximately 256,512 and 117,277 people, accounting for 51.02% and 44.09% of the world's male and female stomach cancer mortality, respectively [1, 2]. The most commonly known causes include *Helicobacter pylori* infection, smoking, and genetic factors. After comprehensive treatment consisting of endoscopic mucosal exfoliation, chemotherapy, radiotherapy and surgery, the prognosis of patients with early-stage GC is favorable. However, for patients with advanced GC or improper treatment in the early stage, the effect of comprehensive treatment is quite poor, and the 5-year survival rate of patients with GC only reaches 21.35% [3]. Even with the current rapid development of medical techniques, the prognosis of patients with GC is still

extremely poor, and further multilevel mechanistic research is urgently needed to improve the early diagnostic rate and investigate more effective treatments. In recent years, advances in tumor molecular pathogenesis studies based on bioinformatics analysis have opened up an important new avenue for tumor research.

Only 2% of RNAs in the human transcriptome encode proteins, and the remaining 98% are noncoding RNAs (ncRNAs) [4, 5], including ribosomal RNAs (rRNAs), long noncoding RNAs (lncRNAs) and microRNAs (miRNAs). Recent advances in next-generation sequencing technologies have led to the identification of previously unidentified and uncharacterized RNA transcripts that have been linked to various growth and development processes, including diseases such as GC. For example, Zhang M et al. indicated that the lncRNA NEAT1 is abnormally overexpressed in patients with breast cancer, and the downregulation of NEAT1 expression prevents the expression of the β-catenin protein, thereby suppressing the hyperplasia and metastasis of breast tumor cells [6]. Su JJ et al. documented that miR-145 is expressed at low levels in patients with colon cancer [7]. Upregulating miR-145 expression silences the target gene IGF1R, thereby inhibiting tumor cell proliferation [7]. Furthermore, researchers also observed a mutual targeting regulatory relationship between different types of ncRNAs [8].

In 2011, Salmena L et al. proposed the concept of competing endogenous RNA (ceRNA), which is defined as a type of RNA that regulates the transcription of other RNAs by competing for shared miRNA binding sites [8]. As a type of ceRNA, lncRNAs regulate the expression levels of mRNAs by competitively sponging miRNAs, affecting the translation of the corresponding proteins and the related cellular activities [8, 9]. Based on this definition, many scientists have hypothesized a "lncRNA/miRNA/mRNA" regulatory mechanism. Based on a large amount of data and experimental verification, many of these regulatory axes have been proposed in GC that are beneficial to clinical treatment research. In 2019, Lu RQ et al. experimentally discovered the HOTAIRM1/miR-17-5p/PTEN axis and proposed the highly expressed lncRNA HOTAIRM1 as a ceRNA that sponged miR-17-5p to mediate the upregulation of PTEN expression and block the PI3K/AKT pathway in GC, thereby suppressing the hyperplasia and metastasis of cancer cells [10]. In 2020, Zhang YM et al. experimentally identified the SNHG7/miR-34a/Snail axis and proposed that the highly expressed lncRNA SNHG7 functioned as the ceRNA of miR-34a to mediate the upregulation of Snail expression and subsequently promote the epithelial-mesenchymal transition (EMT), thereby enhancing the invasiveness and metastasis of GC cells [11]. These studies showed that in gastric cancer, differentially expressed (DE) ceRNAs are closely correlated with the tumorigenesis, progression and prognosis of patients with tumors. Identifying the key points and axes in the ceRNA network may facilitate the identification of new candidate biomarkers or therapeutic targets for the treatment of GC.

In this study, we extracted differentially expressed lncRNAs (DElncRNAs), miRNAs (DEmiRNAs) and mRNAs (DEmRNAs) detected in gastric adenocarcinoma and gastric adenoma samples stored in The Cancer Genome Atlas (TCGA) database. Afterward, using the online tools miRDB, TargetScan and DIANA TOOLS that paired the DERNAs, a ceRNA network was constructed to reveal their inter-targeting and regulatory relationships. Then, we employed the "survival" package of R language to perform a survival analysis of the ceRNA network and identified DERNA-os as related to the patients' five-year survival rate. Finally, "lncRNA/miRNA/mRNA" axes were hypothesized based on the regulatory relationship of DERNA-os in the ceRNA network. On the one hand, the aforementioned DERNA-os and "lncRNA/miRNA/mRNA" axes discovered in this study provide candidate prognostic targets for patients with GC. On the other hand, they might help researchers better understand the role of ceRNAs in gastric tumors, provide new insights for elucidating the molecular mechanisms of GC, and provide a new direction of axial mechanisms for clinical treatment and research.

Materials and methods

Tumor data and differential expression analysis

Data collection from TCGA database: The transcriptome profiles and clinical data of gastric adenocarcinoma and gastric adenoma samples were downloaded from the Genomic Data

Commons Data Portal (GDC, https://portal.gdc.cancer.gov/repository; date: May 2020) in TCGA database. These data contained the following three types of information: 1) RNA sequencing (RNA-seq) data, 2) miRNA sequencing (miRNA-seq) data, and 3) clinical survival time. The acquisition and processing of the data in this study followed the publication guidelines provided by TCGA database. The aforementioned data are freely available to the public; thus, no additional local ethics committee approval was needed.

Identification of DElncRNAs, DEmiRNAs, and DEmRNAs: After data collection and screening, we extracted the miRNA expression matrix from the miRNA-seq profiles, while the lncRNA and mRNA expression matrices were extracted from the RNA-seq profiles. We used the "edgeR" package (DOI: 10.18129/B9.bioc.edge) installed in R software (https://www.r-project.org/, version 3.6.3) using the following screening criteria to further identify the DElncRNAs, DEmiRNAs and DEmRNAs in GC samples: 1) $\log_2$ fold change in expression multiple ($|\log_2 FC|$) > 2.0 and 2) false discovery rate (FDR) < 0.05. The "gplots" package was used to generate heatmaps and volcano plots, where the heatmap illustrated the dysregulation of DERNAs in samples, whereas volcano plots illustrated the top up- and downregulated candidates.

Establishment of the ceRNA network based on DElncRNAs, DEmiRNAs, and DEmRNAs

Prediction of DElncRNA-DEmiRNA and DEmiRNA-DEmRNA pairs: The ceRNA network, which is generated based on experimental data, reveals the relationships between heterogeneous RNAs and may be used to investigate the interactions of multiple RNAs. MiRcode (http://www.mircode.org/) [12] performs a multidirectional prediction of ncRNAs such as lncRNAs and miRNAs. To obtain the DElncRNA-miRNA pairs, we used miRcode to predict the regulatory relationships of DElncRNAs and miRNAs in GC samples. Then, we intersected the miRNAs in these pairs with the DEmiRNAs to identify the relevant DEmiRNAs and obtain the DElncRNA-DEmiRNA pairs in this study.

Likewise, three online analysis tools, miRDB (http://mirdb.org/) [13], TargetScan 7.2 (http://www.targetscan.org/vert_72/) [14], and microT-CDS in DIANA (http://www.microrna.gr/microT-CDS) [15, 16], were employed to predict the target mRNAs of DEmiRNAs in the DEmiRNA-mRNA pairs. Afterward, we screened the intersections of the mRNAs in the aforementioned pairs and the DEmRNAs and obtained the intersecting DEmRNAs and DEmiRNA-DEmRNA pairs in GC samples.

Construction of the ceRNA network: LncRNAs sponge miRNAs and further regulate the expression of the target mRNAs of these miRNAs. In the ceRNA network, miRNAs are the key points connecting lncRNAs and mRNAs. Therefore, we designated miRNA as the center of the ceRNA network and connected the DElncRNA-DEmiRNA pairs and the DEmiRNA-DEmRNA pairs to construct a lncRNA-miRNA-mRNA ceRNA network for GC. Afterward, the ceRNA network was visualized using Cytoscape 3.7.2 software [17]. Additionally, the regulatory relationship in the ceRNA network was further used for the construction of lncRNA/miRNA/mRNA regulatory axes.

Functional enrichment and pathway analysis: We extracted the mRNAs (the target genes) from the ceRNA network and enriched them using the GO and KEGG functional enrichment part in Metascape (http://metascape.org) to explore the cell signaling pathways and biological processes in which mRNAs in the ceRNA network were involved in GC [18]. The resulting GO and KEGG terms with a minimum number of 3 genes, $P < 0.05$, and an enrichment factor > 1.5 were collected. With kappa scores as the similarity metric, hierarchical clustering analysis was performed on the enriched terms, and terms with a similarity > 0.3 were grouped into a cluster that was represented by the most statistically significant term within it. This representative term also covered all genes in the cluster. The top 20 clusters were extracted and rendered as network plots, where terms within the same cluster are connected by edges and the thickness of the edge represents the value of the similarity score.

Identification of tumor prognostic markers and postulated lncRNA/miRNA/mRNA regulatory axes

Identification of tumor prognostic markers among lncRNAs, miRNAs, and mRNAs: We extracted the survival time of the patients who donated the GC samples and used the

"survival" package and "qvalue" package (DOI: 10.18129/B9.bioc.qvalue) in R software to perform a univariate survival analysis of the acquired samples to identify independent prognostic biomarkers in the ceRNA network. In addition, the Kaplan-Meier curve [19] was applied to generate the five-year survival curve of patients with GC. Moreover, at a significance level of $P < 0.05$, prognosis-related tumor markers (DElncRNA-os, DEmiRNA-os and DEmRNA-os) were screened from DElncRNAs, DEmiRNAs and DEmRNAs in the ceRNA network.

Construction of lncRNA/miRNA/mRNA regulatory axes: We first identified the target DEmiRNAs of DElncRNA-os in the ceRNA network and took the intersection of the selected DEmiRNAs and DEmiRNA-os as the DElncRNA-os/DEmiRNA-os pairs to clarify the regulatory relationships between biomarkers in the ceRNA network. Subsequently, we obtained the target DEmRNAs of DEmiRNA-os in the DElncRNA-os/DEmiRNA-os pairs of the ceRNA network and intersected the selected DEmRNAs and DEmRNA-os to obtain the DEmiRNA-os/DEmRNA-os pairs. Afterward, the pairs mentioned above were connected to determine the DElncRNA-os/DEmiRNA-os/DEmRNA-os pairs. In the ceRNA regulatory network, lncRNAs sponge and downregulate miRNAs to subsequently inhibit the expression of their target miRNAs. Similarly, downregulated lncRNAs disinhibit sponged miRNAs, leading to the upregulation of target miRNAs. According to this pattern of regulation, we screened the DElncRNA-os/DEmiRNA-os/DEmRNA-os pairs and predicted the lncRNA/miRNA/mRNA axis in GC.

Data processing

This study adopted R (version 3.6.3) for statistical analysis. The edgeR package in R was employed to obtain the abnormally expressed RNAs. An unpaired two-tailed t test was used to compare the variations between the two groups. $P < 0.05$ was considered statistically significant.

Results

Flow chart of the data mining approach for screening ceRNAs and tumor biomarkers

Figure 1 shows the flow chart of the data mining approach used to screen ceRNAs and tumor biomarkers of GC in this study. R software and various online tools were employed for the analysis. First, we downloaded the expression profiles of lncRNAs, miRNAs and mRNAs in gastric adenocarcinoma and gastric adenoma from TCGA database and obtained DElncRNAs, DEmiRNAs and DEmRNAs after data analysis using R. Then, the miRcode database was used to determine the DElncRNA-DEmiRNA pairs, and miRDB, TargetScan 7.2 and DIANA microT-CDS tools were applied to identify the DEmiRNA-DEmRNA pairs. Thereafter, to visualize the relationship between the two types of pairs, we used Cytoscape to construct a ceRNA network diagram. Furthermore, we used Metascape to conduct an enrichment analysis of mRNAs in the ceRNA network to comprehend the potential functions of the ceRNA network in GC. In addition, through a survival analysis using R, we obtained DElncRNA-os, DEmiRNA-os and DEmRNA-os related to the five-year survival rate of patients. Ultimately, based on the targeting relationships in the ceRNA network, we identified DElncRNA-os/DEmiRNA-os/DEmRNA-os pairs and further predicted the lncRNA/miRNA/mRNA axis according to its regulatory mode. This process is a feasible method to identify potential tumor prognostic biomarkers and predict tumor regulatory axes.

Data extraction and differential expression analysis of lncRNAs, miRNAs and mRNAs

In this study, the data profiles of gastric adenocarcinoma and gastric adenoma were obtained from TCGA database. The profiles included 374 lncRNA samples (normal samples: 30, tumor samples: 344), 453 miRNA samples (normal samples: 42, tumor samples: 411), and 374 mRNA samples (normal samples: 30, tumor samples: 344).

Through a differential expression analysis, 2840 RNAs were identified to be abnormally expressed ($|\log_2 FC| > 2.0$, $P_{-FDR} < 0.05$) in GC samples (**Figure 2Ai-Ci**), consisting of 1052 DElncRNAs (upregulated: 853, downregulated: 199) (**Figure 2Aii**), 102 DEmiRNAs (upregulated: 85, downregulated: 17) (**Figure 2Bii**), and 1686 DEmRNAs (upregulated: 937, downregulated: 749) (**Figure 2Cii**). The red dots denote significantly upregulated RNAs, and the green dots denote significantly downregulated RNAs.

The ceRNA regulatory network of GC

Based on predictions from the miRcode database, we obtained the DElncRNA-DEmiRNA

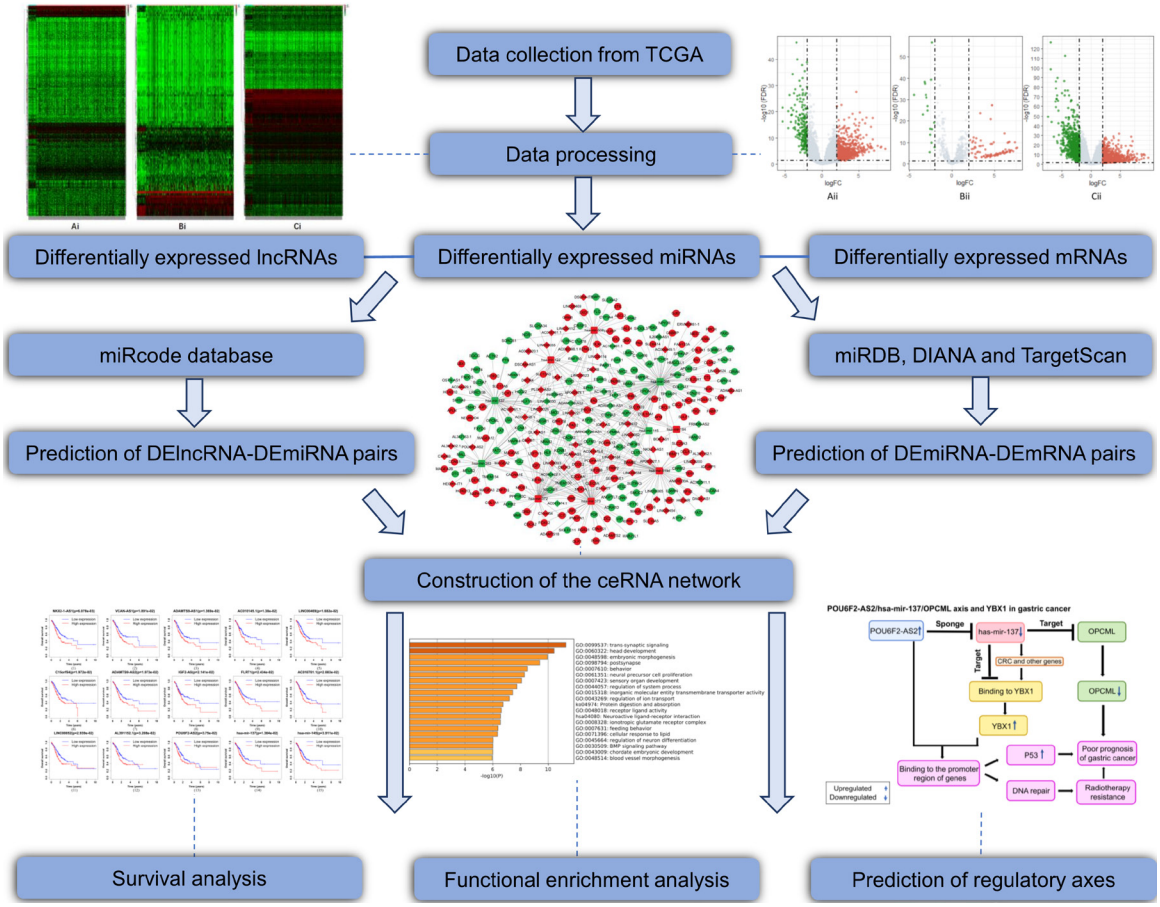

Figure 1. Analysis of prognostic biomarkers and key axes. The analysis includes specific bioinformatics methods, data processing tools, and partial research results.

pairs. According to the screening criteria, 69 DElncRNAs and 10 DEmiRNAs were included in the ceRNA network, and they constituted 154 DElncRNA-DEmiRNA pairs (Supplementary Table 1). Furthermore, three online tools (miRDB, TargetScan 7.2, and DIANA microT-CDS) were employed to predict the target genes of the 10 DEmiRNAs included in the ceRNA network. Thereafter, we intersected the predictions with DEmRNAs; 204 DEmRNAs were included in the ceRNA network, and 288 DEmiRNA-DEmRNA pairs were obtained (Supplementary Table 2).

Finally, based on the DElncRNA-DEmiRNA pairs and DEmiRNA-DEmRNA pairs obtained above, we used Cytoscape to construct the ceRNA network of GC (**Figure 3**). As shown in **Figure 3**, 69 DElncRNAs (upregulated: 51, downregulated: 18), 10 DEmiRNAs (upregulated: 6, downregulated: 4) and 204 DEmRNAs (upregulated: 103, downregulated: 101) were included in the ceRNA network.

GO and KEGG pathway enrichment analyses of 204 mRNAs in the ceRNA network

By performing a functional enrichment analysis of 204 mRNAs in the ceRNA network using the criterion of $P < 0.05$, we obtained the top 20 clusters of GO processes and KEGG pathways (**Figure 4**, Supplementary Table 3), which were represented by the most statistically significant term within them (**Figure 4A**). **Figure 4B** converted the size of the *P value* to the color shade of nodes, where terms containing more genes tended to have a more significant *P value*. **Figure 4C** distinguished different clusters with separate colors, where nodes that share the same cluster ID were typically close to each other. As illustrated in **Figure 4A**, the most significant GO function was the trans-synaptic sig-

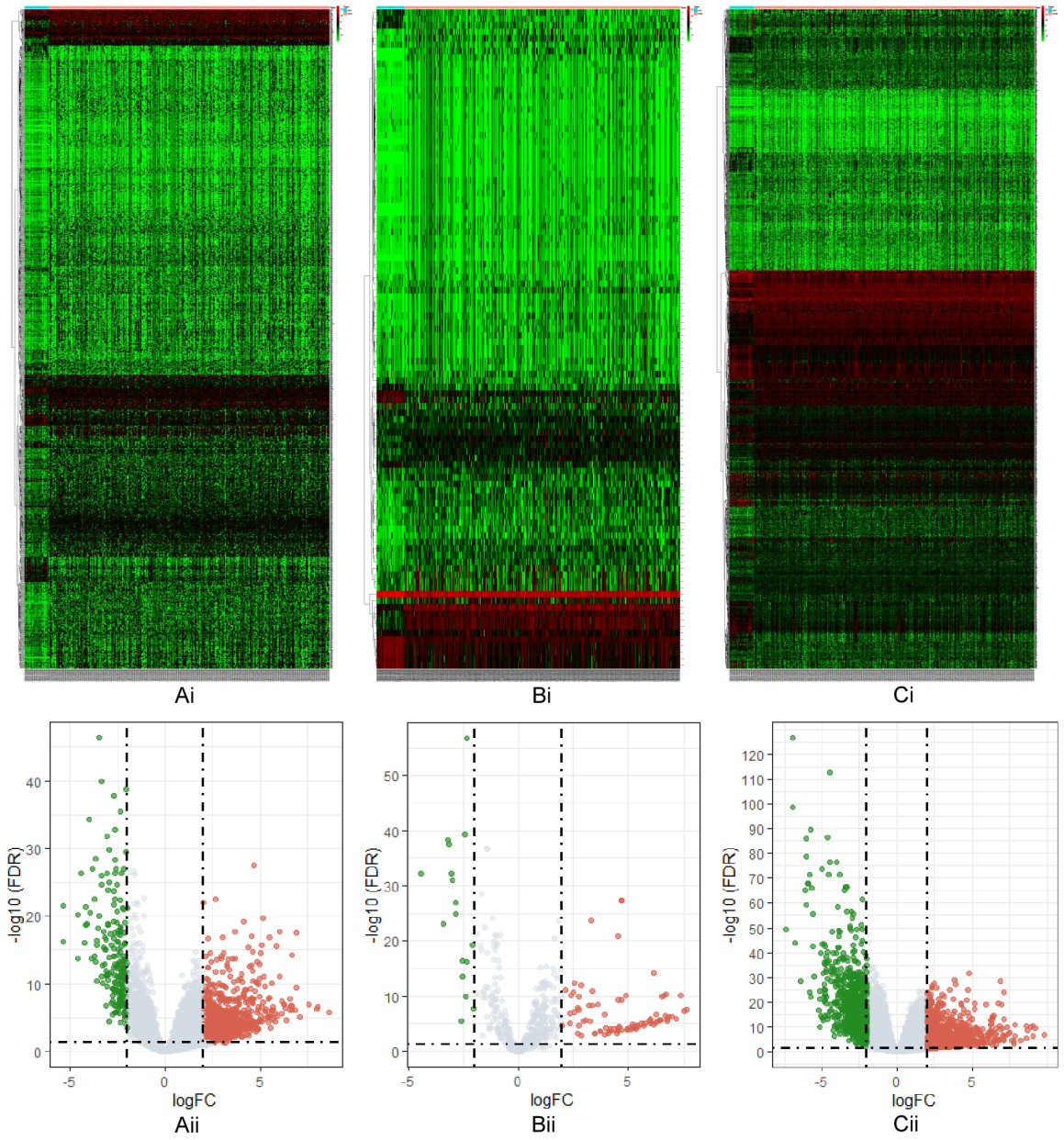

Figure 2. Heatmap and volcano plots of RNAs. With $|\log_2 FC| > 2.0$ and FDR < 0.05 as the standards, heatmaps and volcano plots were drawn to illustrate the outcome of the differential expression analysis. The red dots denote significantly upregulated RNAs, and the green dots denote significantly downregulated RNAs. Ai. Heatmap of lncRNAs; Bi. heatmap of miRNAs; Ci. heatmap of mRNAs. The abscissa represents the log2 transformation value of the fold change in differential expression between GC samples and normal samples. The larger the $|\log_2 FC|$ value, the greater the fold change. The ordinate represents the -log10 transformation of the FDR value. The larger the -log10 transformation value, the more significant the difference. Aii. Volcano plot of lncRNAs; Bii. volcano plot of miRNAs; Cii. volcano plot of mRNAs. The abscissa represents logFC, where the farther the point deviates from the center, the greater the fold change; the negative half represents downregulation, and the positive half represents upregulation. The ordinate represents -log (FDR), where the closer the point is to the top, the more significant the difference in expression between GC samples and normal samples.

naling cluster. Among the top 20 clusters, 2 KEGG functional pathway clusters, the protein digestion and absorption cluster and neuroactive ligand-receptor interaction cluster, were identified, and the former was more statistically significant than the latter.

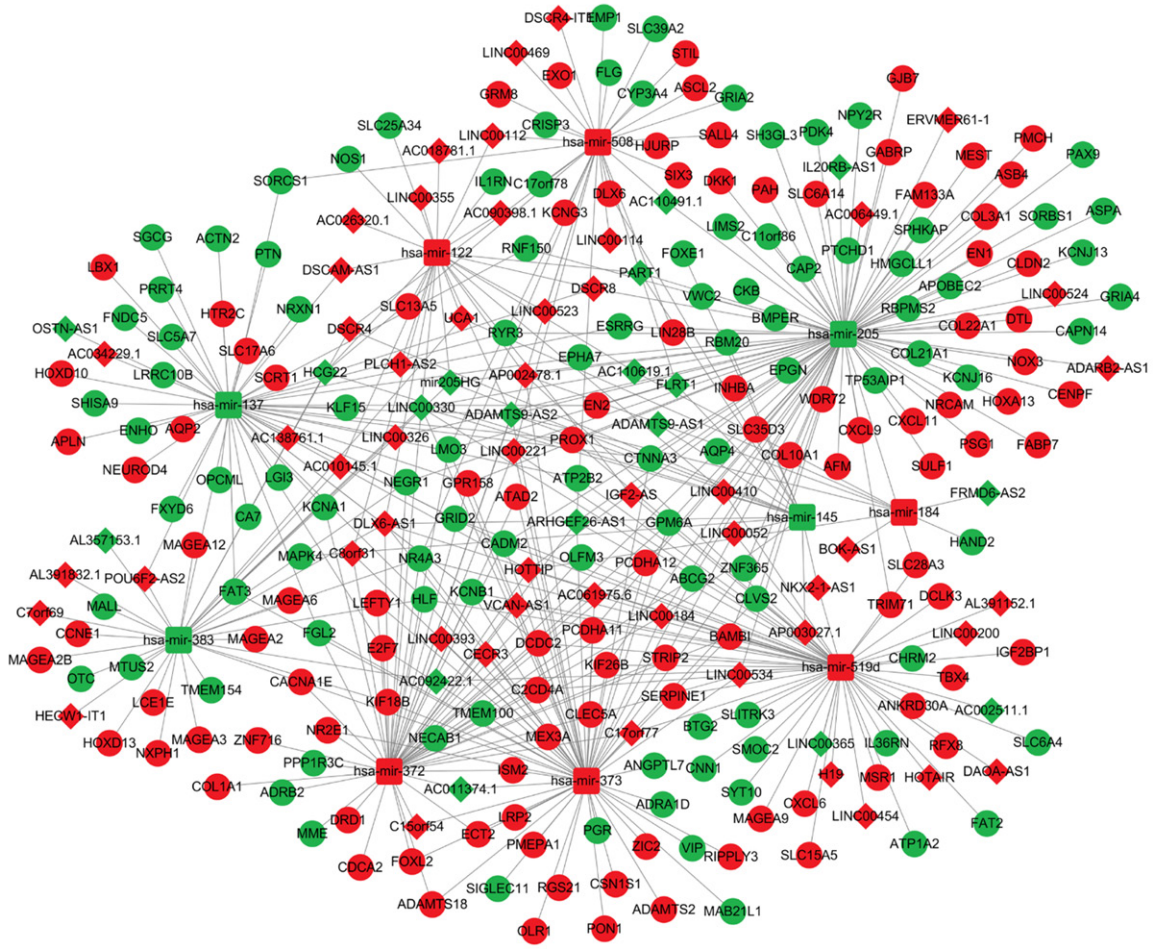

Figure 3. The ceRNA network diagram. Red indicates upregulated RNA expression, green indicates downregulated RNA expression, diamonds represent lncRNAs, squares represent miRNAs, and circles represent mRNAs. 69 DElncRNAs, 10 DEmiRNAs and 204 DEmRNAs were included in the network. They targeted each other and paired to form 154 DElncRNA-DEmiRNA pairs and 288 DEmiRNA-DEmRNA pairs.

Prognostic tumor markers and regulatory axes of GC

13 DElncRNA-os, 2 DEmiRNA-os, and 28 DEmRNA-os prognostic tumor markers: According to the results of the survival analysis with $P < 0.05$ as the level of significance, we identified the following RNAs in the ceRNA network: 1) NKX2-1-AS1, VCAN-AS1 and 11 other DElncRNA-os prognostic tumor markers (**Figure 5A-M**); 2) hsa-mir-137 and hsa-mir-145 as the DEmiRNA-os prognostic tumor markers (**Figure 5N**, **5O**); and 3) *Homo sapiens* serpin family E member 1 (SERPINE1), a disintegrin and metalloproteinase with thrombospondin motifs 18 (ADAMTS18) and 26 other DEmRNA-os prognostic tumor markers (Supplementary Figure 1). **Table 1** presents changes in the expression of the 43 prognostic tumor markers listed above, among which 25 were upregulated and 18 were downregulated.

Among the 13 DElncRNA-os and 2 DEmiRNA-os prognostic biomarkers, the overexpression of five DElncRNA-os (NKX2-1-AS1, VCAN-AS1, IGF2-AS, LINC00052, and POU6F2-AS2), the downregulation of one DElncRNA-os (ADAMTS9-AS2) and two DEmiRNA-os (hsa-mir-137 and hsa-mir-145) were confirmed in previous experimental studies of GC (**Tables 2**, **3**). In addition, the downregulation of DElncRNA-os ADAMTS9-AS1 was reported in earlier experimental prostate cancer studies (**Table 2**). The abnormal expression of the remaining six DElncRNA-os (upregulated: C15orf54; AC018781.1, AL391152.1, AC010145.1, and LNC00469, down-

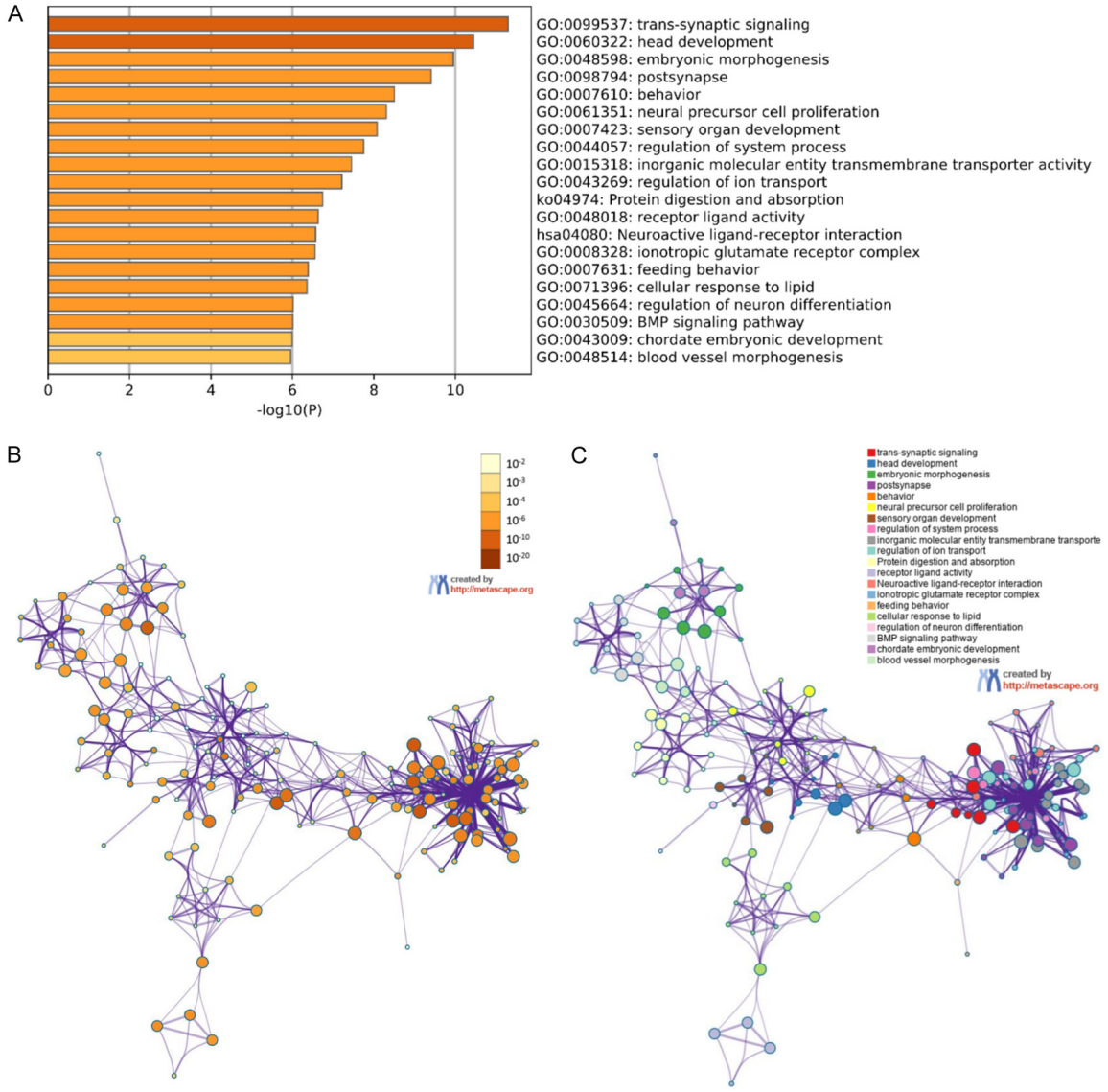

Figure 4. Functional enrichment analysis of 204 mRNAs. A. Bar graph of enriched terms across input gene lists colored by *P value*s. B. Network of enriched terms colored by *P value*, where terms containing more genes tend to have a more significant *P value*. C. Network of enriched terms colored by cluster ID, where nodes that share the same cluster ID are typically close to each other.

regulated: FLRT1) has not been verified in any experimental studies of cancer before. However, the upregulation of three of them (C15orf54, AL391152.1 and AC018781.1) and the downregulation of the final one (FLRT1) were reported by previous data mining studies on GC (**Tables 2**, **3**).

Of the 28 DemRNA-os prognostic gene markers, the upregulation of 12 mRNAs (SERPINE1, ADAMTS18, INHBA, CXCL9, OLR1, HOXA13, COL3A1, STIL, COL10A1, KIF18B, ATAD2, and DKK1) and the downregulation of 4 mRNAs (FAT3, LIMS2, OPCML, and RBPMS2) were confirmed by previous experimental studies of GC. In addition, the upregulation of 1 mRNA (DCLK3) and the downregulation of 3 mRNAs (ASPA, COL21A1, and FXYD6) were confirmed in experimental studies on other cancers. However, the high expression level of 1 mRNA (PDK4) in GC cell lines and the low expression level of 3 mRNAs (NECAB1, ADRA1D, and SLITRK3) in other cancers were reported in previous studies, which differed from the results of our study.

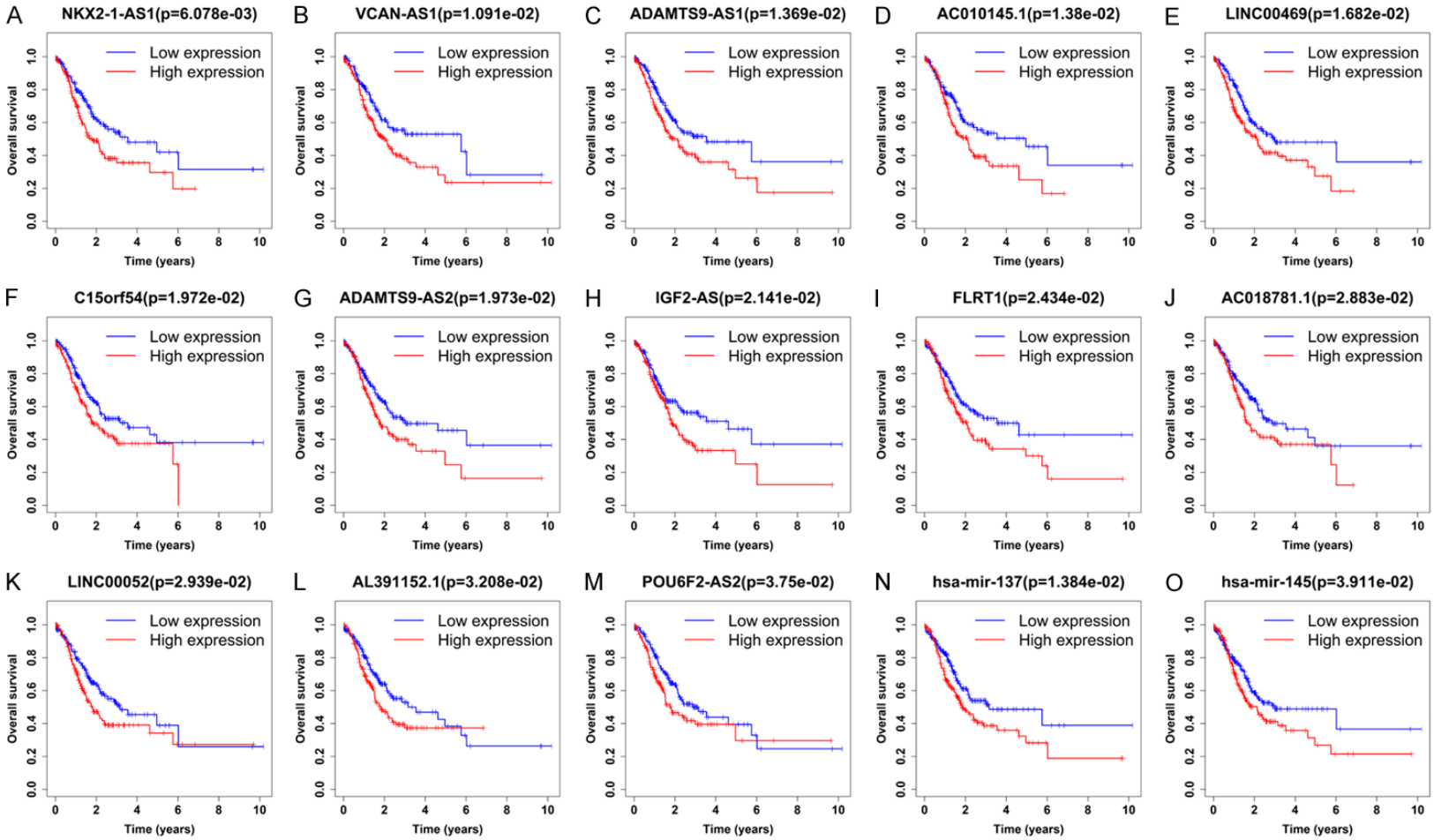

Figure 5. Survival curves of lncRNAs and miRNAs in the ceRNA network. (A-M) show the survival curves of 13 lncRNAs, while (N and O) show the survival curves of 2 miRNAs. The x-axis represents overall survival time, and the y-axis represents the overall survival rate. $P < 0.05$ is considered statistically significant.

Table 1. Prognostic lncRNA, miRNA, and mRNA biomarkers in the ceRNA network

RNA	Change in Expression	Name	$P_{-adj.}$
lncRNA	Upregulated	NKX2-1-AS1	6.08E-03
		VCAN-AS1	1.02E-02
		AC010145.1	1.38E-02
		LINC00469	1.68E-02
		C15orf54	1.97E-02
		IGF2-AS	2.14E-02
		AC018781.1	2.88E-02
		LINC00052	2.94E-02
		AL391152.1	3.21E-02
		POU6F2-AS2	3.75E-02
	Downregulated	ADAMTS9-AS1	1.37E-02
		ADAMTS9-AS2	1.97E-02
		FLRT1	2.43E-02
miRNA	Downregulated	hsa-mir-137	1.38E-02
		hsa-mir-145	3.91E-02
mRNA	Upregulated	SERPINE1	1.19E-03
		ADAMTS18	2.38E-03
		PCDHA11	8.61E-03
		INHBA	1.54E-02
		DCLK3	1.95E-02
		PCDHA12	2.04E-02
		CXCL9	2.25E-02
		OLR1	3.60E-02
		HOXA13	3.70E-02
		COL3A1	4.02E-02
		STIL	4.02E-02
		COL10A1	4.04E-02
		KIF18B	4.42E-02
		ATAD2	4.46E-02
		DKK1	4.70E-02
	Downregulated	NECAB1	4.36E-03
		FAT3	4.37E-03
		PDK4	5.05E-03
		ZNF365	8.78E-03
		LIMS2	1.02E-02
		ASPA	1.51E-02
		PRRT4	2.09E-02
		COL21A1	3.10E-02
		FXYD6	3.96E-02
		OPCML	4.14E-02
		ADRA1D	4.37E-02
		RBPMS2	4.38E-02
		SLITRK3	4.92E-02

The abnormal expression of the remaining 4 mRNAs (upregulated: PCDHA11 and PCDHA12; downregulated: ZNF365 and PRRT4) has not been verified in any experimental studies of cancer before, while the methylation of ZNF365 was experimentally reported to be associated with GC, the mutation of PCDHA11 has been informed by a sequencing analysis of large granular lymphocyte leukemia and the downregulation of PCDHA12 was shown in a previous data mining study on squamous cell lung cancer (**Table 4**).

Four lncRNA/miRNA/mRNA regulatory axes based on the ceRNA network: As shown in **Figure 6**, according to the regulatory relationships of RNAs included in the ceRNA network, the 13 DElncRNA-os and 2 DEmiRNA-os described above formed 7 DElncRNA-os/DEmiRNA-os pairs (ADAMTS9-AS2/hsa-mir-137, FLRT1/hsa-mir-137, POU6F2-AS2/hsa-mir-137, ADAMTS9-AS1/hsa-mir-145, ADAMTS9-AS2/hsa-mir-145, LINC00052/hsa-mir-145, and NKX2-1-AS1/hsa-mir-145). Likewise, the 2 DEmiRNA-os and 28 DEmRNA-os listed above formed 4 DEmiRNA-os/DEmRNA-os pairs (hsa-mir-137/OPCML, hsa-mir-137/FXYD6, hsa-mir-137/FAT atypical cadherin 3 (FAT3), and hsa-mir-137/proline-rich transmembrane protein 4 (PRRT4)).

Afterward, with DEmiRNA-os as the connection point, we combined the DElncRNA-os/DEmiRNA-os pairs and the DEmiRNA-os/DEmRNA-os pairs to obtain 12 DElncRNA-os/DEmiRNA-os/DEmRNA-os interactions. According to the criterion that lncRNAs should downregulate miRNA expression, eight DElncRNA-os/DEmiRNA-os/DEmRNA-os interactions were further discarded, and we finally obtained four lncRNA/miRNA/mRNA axes (POU6F2-AS2/hsa-mir-137/OPCML, POU6F2-AS2/hsa-mir-137/FXYD6, POU6F2-AS2/hsa-mir-137/FAT3, and POU6F2-AS2/hsa-mir-137/PRRT4) that might affect the prognosis and progression of GC (**Figure 6**). Some of the components and regulatory relationships in these axes were supported by earlier experiments on cancer (**Table 5**). In **Figure 7A**, we used the POU6F2-AS2/hsa-mir-137/OPCML axis as an example, in which overexpressed POU6F2-AS2 sponged and downregulated hsa-mir-137, further leading to the low expression of the target gene OPCML. The corresponding experimental evidence for each part of the axis is shown in the box in **Figure 7B** to help readers understand the potential mechanism. The derivation of this ceRNA axis is fully discussed in the Discussion section.

Table 2. Comparison of the abnormal changes in the expression of 13 lncRNAs identified in this study and previous experimental studies on cancer

Number	lncRNA	Feature	Study findings	Citation
1	NKX2-1-AS1	▲	qRT-PCR and immunohistochemical staining indicated that the upregulation of NKX2-1-AS1 in GC tissues downregulated the sponged miR-145-5p, then upregulated SERPINE1, and further promoted proliferation, invasion, metastasis, and angiogenesis of tumor cells via stimulating the VEGFR-2 signaling pathway.	[42]
2	VCAN-AS1	▲	Analyses of clinical samples, TCGA database samples and in vitro cell-based experiments revealed that VCAN-AS1 was upregulated in GC tissues and cells, and silencing VCAN-AS1 inhibited the proliferation, invasion and metastasis of cancer cells.	[43]
3	IGF2-AS	▲	qRT-PCR and immunohistochemical detection revealed that the upregulation of IGF2-AS in GC tissues downregulated the expression level of the sponged miR-503, led to the upregulation of SHOX2, and promoted the progression and metastasis of GC.	[44]
4	LINC00052	▲	Detection of clinical samples and in vitro cell-based experiments showed that the abnormally high expression of LINC00052 in GC samples interacted with SMYD2 methyltransferase and then stimulated β-catenin methylation to activate the Wnt/β-catenin pathway, subsequently promoting the hyperplasia and migration of GC cells.	[45]
5	POU6F2-AS2	▲	RT-qPCR confirmed that POU6F2-AS2 was expressed at higher levels in GC samples than in matched adjacent normal samples.	[46]
6	ADAMTS9-AS2	▼	qRT-PCR and in vitro cell culture experiments showed that the lncRNA ADAMTS9-AS2 was expressed at low levels in GC cells. Upregulating ADAMTS9-AS2 expression in the MKN45 cell line stimulated the expression of SPOP to further inhibit the proliferation of GC cells and the tumorigenicity of tumor stem cells.	[47]
7	ADAMTS9-AS1	▽	The qRT-PCR assay showed that ADAMTS9-AS1 expression was downregulated in prostate cancer tissues and cells, and the upregulation of ADAMTS9-AS1 expression in prostate cancer cells downregulated the sponged hsa-mir-96, thus indirectly upregulating the expression of PRDM16 and subsequently inhibiting the proliferation of cancer cells.	[48]
8	C15orf54	△	The overexpression of C15orf54 has not been mentioned in any cancer experiments. However, a data mining study of gastric adenocarcinoma suggested that C15orf54 was upregulated in tumor samples and was included in a multivariable Cox risk model designed to predict the prognosis of patients with GC.	[46]
9	AC018781.1	△	The abnormally high expression of AC018781.1 has not been mentioned in any cancer experiments. However, a data mining study of gastric adenocarcinoma suggested that AC018781.1 was downregulated in tumor samples and was a predicted independent prognostic factor for GC.	[46]
10	AL391152.1	△	The abnormally high expression of AL391152.1 has not been mentioned in any cancer experiments. Nevertheless, a data mining study of gastric adenocarcinoma suggested that AL391152.1 was upregulated in tumor samples and was included in a multivariable Cox risk model designed to predict the prognosis of patients with GC.	[46]
11	AC010145.1	△	AC010145.1 is a biomarker reported for the first time in the present study. We found that abnormally high expression of AC010145.1 was significantly related to a poor prognosis for patients with GC.	\
12	LINC00469	△	LINC00469 is a biomarker reported for the first time in the present study. We found that abnormally high expression of LINC00469 was significantly related to a poor prognosis for patients with GC.	\
13	FLRT1	▽	The abnormally low expression of FLRT1 has not been mentioned in any cancer experiments. However, in a data mining study of in gastric adenocarcinoma, the Kaplan-Meier survival analysis revealed decreased FLRT1 expression in patients with GC, and its hypermethylation was significantly related to the poor prognosis of these patients.	[49]

Notes: ▲ a lncRNA experimentally upregulated in GC in accord with our calculated results; ▼ a lncRNA experimentally downregulated in GC in accord with our calculated results; ▽ a lncRNA experimentally downregulated in other cancers in accord with our calculated results; △ a lncRNA upregulated in our calculated results that has not been experimentally verified in GC or other cancers; ▽ a lncRNA downregulated in our calculated results that has not been experimentally verified in GC or other cancers.

Table 3. Comparison of the abnormal changes in miRNA expression identified in this study and previous experimental studies of cancers

miRNA	Number	Feature	Study findings	Citation
miR-137	1	▼	Wu LP et al. reported significantly reduced expression of miR-137 in GC cell lines. Overexpressed miR-137 reduced GC cell proliferation and metastasis by regulating AKT2-related signal pathways.	[50]
	2	▼	Deng J et al. reported decreased expression of miR-137 in GC cells lines. The overexpression of miR-137 significantly suppressed the proliferation and invasion of GC cells.	[51]
miR-145	3	▼	Lei C et al. confirmed that the expression of miR-145 was downregulated in GC cells. Overexpressed miR-145 suppressed GC cell migration and metastasis by inhibiting the EMT.	[52]
	4	▼	Zeng JF et al. indicated that miR-145 was downregulated in cancer tissues and cells. Upregulated miR-145 negatively regulated the migration and metastasis of GC cells.	[53]

Notes: ▼ a miRNA experimentally downregulated in gastric cancer in accord with our calculated results.

Table 4. Comparison of changes in the expression of 28 mRNAs identified in this study and previous experimental studies on cancer

Number	mRNA	Feature	Study findings	Citation
1	SERPINE1	▲	By analyzing samples in TCGA database and cells in vitro, SERPINE1 was shown to be expressed at high levels in patients with gastric adenocarcinoma and cancer cells. Silencing SERPINE1 inhibited the EMT process, thereby inhibiting the proliferation and metastasis of gastric adenocarcinoma cells.	[54]
2	ADAMTS18	▲	Immunohistochemical analysis of clinical tissue samples showed that ADAMTS18 was expressed at high levels in GC tissues and was significantly related to a high tumor stage.	[55]
3	INHBA	▲	Detection of clinical samples and in vitro cell-based experiments indicated that INHBA was expressed at high levels in patients with GC and cancer cells. Silencing INHBA inactivated the TGF-β signaling pathway and inhibited the metastasis and invasion of GC cells.	[56]
4	CXCL9	▲	An analysis of samples from TCGA database and cell culture experiments revealed that CXCL9, which was abnormally highly expressed in GC tissues, increased the expression of PD-L1 in GC cells and tissues by activating the STAT and PI3K-Akt pathways, and participated in promoting the immune escape of cancer cells.	[57]
5	OLR1	▲	Tissue detection and experiments with cell lines indicated that OLR1, also known as LOX1, was upregulated in GC cells. Overexpression of LOX1 drove the EMT and activated the PI3K/Akt/GSK3β pathway, therefore facilitating the metastasis of GC cells.	[58]
6	HOXA13	▲	An analysis of gene microarray data revealed that HOXA13 was expressed at high levels in GC tissues and was associated with advanced stage GC. Cell-based experiments confirmed that the upregulation of HOXA13 expression activated the TGF-β pathway in GC cells, promoted the EMT process, and increased the invasion and metastasis of cancer cells.	[59]
7	COL3A1	▲	A gene expression microarray analysis of tissue samples from patients with GC and mice revealed that COL3A1 was abnormally highly expressed in GC tissues and was involved in activating the MYC, STAT3 and β-catenin (CTNNB1) transcription network and promoting the occurrence and progression of gastric cancer.	[60]
8	STIL	▲	Analyses of clinical samples, samples from TCGA database and cells in vitro illustrated that STIL, which was expressed at high levels in GC tissues and cells, enhanced the activity of the IGF-1/PI3K/AKT signaling pathway, and promoted the proliferation of GC cells and the growth of GC in vivo.	[61]
9	COL10A1	▲	Analyses of clinical samples, mouse experiments and cell culture in vitro indicated that COL10A1, which was upregulated in GC tissues, upregulated SOX9 expression by activating the TGF-β1 signaling pathway and promoted the invasion and metastasis of GC cells.	[62]
10	KIF18B	▲	qRT-PCR and flow cytometry experiments illustrated that KIF18B was highly expressed in gastric cancer cells. The upregulation of KIF18B significantly enhanced the proliferation, migration and invasion abilities of stomach cancer cells.	[63]
11	ATAD2	▲	qRT-PCR and immunohistochemical detection of clinical tissues showed that ATAD2 was expressed at high levels in GC and was significantly related to the clinical stage, poor prognosis, deep tumor invasion, lymph node metastasis, and distant metastasis of GC.	[64]
12	DKK1	▲	Immunohistochemical staining of GC clinical specimens revealed that the abnormally high expression of DKK1 in GC samples might be useful as an independent marker for the poor prognosis of patients with GC.	[65]
13	FAT3	▼	Cell-based experiments indicated that knocking out MEF2C-AS1 or FENDRR in GC cell lines further reduced the level of FAT3 and other proteins related to GC cell proliferation and invasion and promoted the proliferation of GC cells.	[66]
14	LIMS2	▼	qRT-PCR and immunohistochemical detection of GC clinical tissue specimens revealed that LIMS2 was expressed at low levels in GC tissues and cells. Cell-based experiments indicated that its downregulation was related to CpG island hypermethylation, and the low expression of LIMS2 promoted cancer cell migration.	[67]
15	OPCML	▼	Through the detection of clinical GC samples and cell-based experiments, the authors verified that OPCML was expressed at low levels in GC tissues and cells. Upregulating OPCML expression inhibited the growth and colony formation of GC cells, arrested the cells in G0/G1 phase, and promoted cancer cell apoptosis.	[68]
16	RBPMS2	▼	Immunohistochemical detection of tumor cells at the tumor center and at the invasive front of resected GC tissue manifested that low expression of RBPMS2 was more frequent at the invasive front (57.7%), which was associated with the nonintestinal type and positive lymphatic invasion ($P < 0.01$).	[69]
17	PDK4	⚠	By performing experiments using GC tissues and cells, PDK4 was shown to be overexpressed in cancer cells. Downregulation of miR-5683 disinhibited glycolysis by upregulating PDK4 in GC cells.	[70]
18	DCLK3	⚠	According to a proteome-wide analysis of disease-associated SNPs (PWAS) and analysis of cell-based experiments of colon cancer, transcription factors bound to the MLH1 rs1800734 A allele to enhance the chromatin interaction between the rs1800734 locus and the DCLK3 region and further upregulated the expression of DCLK3, thereby promoting the EMT process of cancer cells and increasing the malignancy of colon cancer.	[71]

19	ASPA	▽	Assessments of glioma tissue samples and cell experiments revealed that ASPA is expressed at low levels in glioma cells, and glioma stem cell-like cells promote ASPA expression to maintain their undifferentiated state.	[72]
20	COL21A1	▽	A qRT-PCR assay of clinical tissue samples from patients with head and neck cancer showed that COL21A1 was abnormally repressed in head and neck cancer tissues, and its expression was downregulated up to 4-fold compared with that in matched normal tissues.	[73]
21	FXYD6	▽	Colorectal cancer (CRC) samples and cell-based experiments showed that FXYD6 was abnormally expressed at low levels in CRC patients with drug-resistant and irinotecan-resistant SW620 cells. FXYD6 knockdown decreased the activity of ATP-α1, inhibited cell autophagy and apoptosis, therefore inducing irinotecan and oxaliplatin resistance.	[74]
22	NECAB1	◬	Immunohistochemical detection of clinical tissue samples from patients with thyroid cancer indicated that NECAB1 (also known as STIP-1) was expressed at high levels in cancer tissues and was significantly related to the thyroid cancer tumor size, multiple foci, vascular invasion, and distant metastasis.	[75]
23	ADRA1D	◬	Detection of clinical prostate cancer samples and analyses of cell-based experiments revealed ADRA1D was highly expressed in prostate tissue, and silencing ADRA1D inhibited the proliferation of cancer cells mediated by norepinephrine.	[76]
24	SLITRK3	◬	qRT-PCR and immunohistochemical detection of clinical tissue samples illustrated that the expression of SLITRK3 was upregulated in gastrointestinal stromal tumor tissue, and it was closely related to the long-term survival rate and tumor-free survival rate of patients.	[77]
25	PCDHA11	△	The abnormally upregulation of PCDHA12 has not been reported in any cancer experiments. However, a whole exome and transcriptome sequencing analysis on large granular lymphocyte leukemia indicated that PCDHA11 was a recurrently mutated putative driver of leukemia.	[78]
26	PCDHA12	△	The abnormally high expression of PCDHA12 has not been reported in any cancer experiments. However, in a data mining study of squamous cell lung cancer, the Cox risk prediction model composed of downregulated PCDHA12 and 6 other genes predicted patient prognosis.	[79]
27	ZNF365	▽	The abnormally low expression of ZNF365 has not been mentioned in any cancer experiments. Nevertheless, through an experimental analysis of GC samples and cells, the ZNF365 gene was shown to be methylated in EBV+ and EBV−/high methylation tumors groups.	[80]
28	PRRT4	▽	PRRT4 is a biomarker reported for the first time in the present study. We found that downregulation of PCDHA11 expression was significantly related to a poor prognosis for patients with GC.	\

Notes: ▲ An mRNA upregulated experimentally in GC in accord with our calculated results; ▼ An mRNA experimentally downregulated in GC in accord with our calculated results; ◬ An mRNA experimentally upregulated in GC which different from our calculated results; ▽ An mRNA experimentally downregulated in GC which different from our calculated results; △ An mRNA experimentally upregulated in other cancers in accord with our calculated results; ▽ An mRNA experimentally downregulated in other cancers in accord with our calculated results; ◬ An mRNA experimentally upregulated in other cancers which differ from our calculated results in GC; ▽ An mRNA experimentally downregulated in other cancer which differ from our calculated results in GC; △ An mRNA upregulated in our calculated results that has not been experimentally verified in GC or other cancers; ▽ An mRNA downregulated in our calculated results that has not been experimentally verified in GC or other cancers.

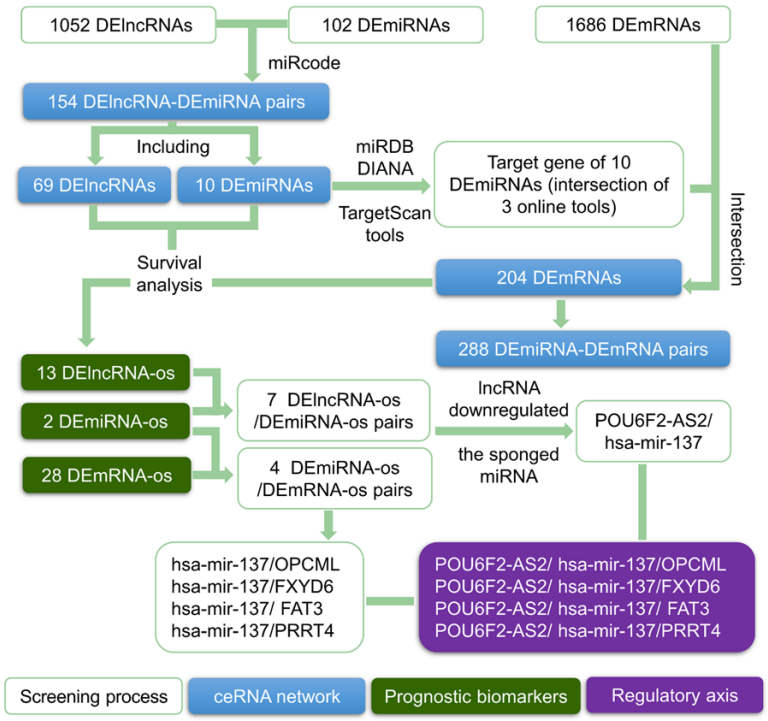

Figure 6. Establishment of 4 lncRNA/miRNA/mRNA axes. The blank rectangles represent the screening process, the blue rectangles represent the components of the ceRNA network, the green rectangles represent candidate prognostic targets, and the purple rectangles represent the regulatory axes.

Discussion

GC is one of the most common malignancies in the world [1]. In China, stomach cancer ranked second in incidence and third in cancer-related mortality in 2021 [2]. The 5-year survival rate of patients with GC is less than 21.35% due to the lack of effective treatments in the advanced stage [3]. Therefore,

Table 5. Supporting evidence for lncRNA/miRNA/mRNA regulatory axes

Number	Components	Circumstantial Evidence	References
1	POU6F2-AS2 and YBX1	Liu J et al. reported that in squamous cell esophageal cancer samples, POU6F2-AS2 targets and binds YBX1, which is indispensable for the binding of YBX1 to chromatin. In addition, YBX1 compensates for the function of POU6F2-AS2 in repairing DNA damage in response to ionizing radiation treatment, which leads to treatment failure and undesirable outcomes. POU6F2-AS2 knockout inhibits YBX1 locating at and binding to damaged DNA, which further increases the amount of DNA damage in cancer cells and improves the radiotherapy sensitivity of cancer tissues.	[31]
2	hsa-mir-137 and YBX1	Chu PC et al. showed that high miR-137 expression in CRC inhibits YBX1 expression by targeting the 3'UTR of YBX1. Johnson TG et al. observed that transfection of miR-137 analogs inhibits the growth, metastasis and invasion of malignant pleural mesothelioma cells, and this process is related to the direct downregulation of YBX1 expression.	[32, 33]
3	hsa-mir-137 and FXYD6	Li ZM et al. reported that FXYD6 is directly targeted and downregulated by the upregulation of miR-137. When FXYD6 is upregulated, the tumor-suppressive effects of overexpressed miR-137 on osteosarcoma migration and proliferation are reversed.	[81]

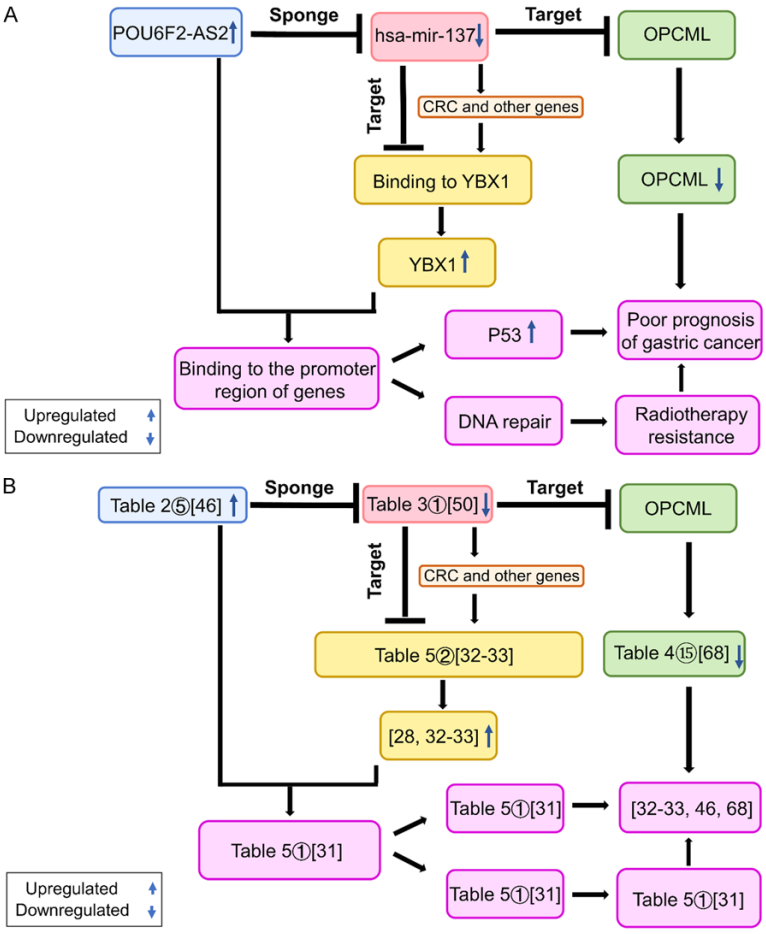

Figure 7. Mechanism plot (A) and evidence map (B) of the POU6F2-AS2/hsa-mir-137/OPCML axis and YBX1 in gastric cancer.

the early detection of GC is essential for the treatment of patients and for a maximized therapeutic effect. With the progress in bioinformatics research in cancers, including gastric carcinoma, a variety of RNA biomarkers related to tumor proliferation, metastasis, invasion, and prognosis have been identified [20-22]. These RNAs contribute to guiding clinical treatment decisions, predicting patient prognosis and developing personalized treatment for patients.

Notably, ncRNA is commonly recognized as a type of RNA that does not encode protein. However, ncRNAs have been reported to possess biological functions such as transcriptional regulation, RNA splicing and modification, and chromosome stabilization [23]. NcRNAs can be divided into small ncRNAs (sncRNAs, including miRNAs), lncRNAs and circular RNAs (circRNAs) according to their size. Studies have shown that in addition to regulating the carcinogenesis and progression of many cancers, ncRNAs also target and regulate other ncRNAs [8, 9]. This type of ncRNA is called a ceRNA, and the network formed through their regulatory relationships is called a ceRNA network [8, 9]. The ceRNA network is based on the concept that mRNAs, pseudogene transcripts and lncRNAs use miRNA response elements (MREs) as binding targets to "talk" to each other and to target and regulate the expression of one another [8]. Among them, lncRNAs function as miRNA sponges to com-

petitively inhibit sponged miRNAs [24, 25]. MiRNAs inhibit the translation of target mRNAs or mediate the deadenylation and degradation of target mRNAs, thus reducing protein synthesis [26]. Emerging evidence shows that lncRNAs sponge miRNAs to further regulate the expression of target mRNAs and then participate in the carcinogenesis, progression and metastasis of cancer [24, 25]. This process occurs through the lncRNA/miRNA/mRNA regulatory axis based on the ceRNA network. In this paper, we analyzed the regulatory mechanisms between the components of this axis and discussed the involved target signals and protein pathways to further study the mechanisms of GC carcinogenesis and progression.

Our study is based on 453 miRNA samples, 374 lncRNA samples and 374 mRNA samples from TCGA database related to gastric adenocarcinoma and gastric adenoma. By performing differential expression analyses, we first identified 1052 DElncRNAs (853 upregulated and 199 downregulated), 102 DEmiRNAs (85 upregulated and 17 downregulated), and 1686 DEmRNAs (937 upregulated and 749 downregulated). Then, we detected the DERNA interacting pairs (Supplementary Tables 1, 2) using miRcode, miRDB, TargetScan and DIANA TOOLS. Finally, based on these pairs, we constructed a ceRNA network consisting of 69 lncRNAs, 10 miRNAs and 204 mRNAs. Among them, 43 ncRNAs were related to survival (13 lncRNAs, 2 miRNAs, and 28 mRNAs).

After a thorough literature search and careful analysis of the 43 candidate prognostic RNAs, we found that 17 overexpressed RNAs (5 lncRNAs and 12 mRNAs) and 7 downregulated RNAs (1 lncRNA, 2 miRNAs, and 4 mRNAs) have been experimentally confirmed to promote the progression and invasion of tumor cells in previous GC studies, denoting that at least 55.81% (24 of 43) biomarkers were predicted successfully by our calculation (**Tables 2**-**4**). In addition, the upregulation of 1 RNAs (1 mRNAs) and the downregulation of 4 RNAs (1 lncRNA and 3 mRNAs) have been documented to stimulate a significant process of tumor cells in previous experiments on other cancers, indicating that 11.63% (5 of 43) of biomarkers might also be predicted correctly (**Tables 2** and **4**). On the other hand, the abnormal expression of 4 mRNAs (1 downregulated and 3 upregulated) was predicted in the opposite direction from previous experimental reports; however, only one of these four mRNAs (PDK4) was indeed studied in GC (**Table 4**). Finally, 10 RNAs (6 lncRNAs and 4 mRNAs) have not been confirmed by any previous experiments. Among the 10 RNAs, the predictions of dysregulation of 3 RNAs (2 upregulated lncRNAs and 1 downregulated lncRNA) in this study were consistent with those from other data mining studies, while the prediction of the abnormal upexpression of 1 lncRNA (AC018781.1) and 1 mRNA (PCDHA12) here were opposite to those from other calculation studies. One mRNA was reported to be methylated in gastric cancer cells, 1 mRNA was identified as a mutation driver in large granular lymphocyte leukemia cells and 3 RNAs (2 lncRNAs: AC010145.1 and LNC00469; 1 mRNA: PRRT4) were novel potential prognostic biomarkers that had never been reported before, signifying that our study had an at least 6.98% prediction capability (**Tables 2** and **4**). Moreover, because these experimentally unconfirmed RNAs may have different functions in different cancers or even in different subtypes and stages of GC, 44.19% (19 of 43) of biomarkers may be aggressively regarded as prognostic. Therefore, we believe that this calculation work is valuable because of its showing both strong reliability and predictability.

Based on the ceRNA target-relationship network, we obtained four lncRNA/miRNA/mRNA regulatory axes (POU6F2-AS2/hsa-mir-137/OPCML, POU6F2-AS2/hsa-mir-137/FAT3, POU6F2-AS2/hsa-mir-137/FXYD6, and POU6F2-AS2/hsa-mir-137/PRRT4) from 43 DERNA-os that might affect the progression of GC. None of the four axes have been reported in previous studies, yet their components have appeared in different experimental reports on cancer. The high expression of POU6F2-AS2 and the low expression of hsa-mir-137, OPCML and FAT3 were previously experimentally confirmed in GC. Low expression of FXYD6 has not been reported to be related to GC, but its low expression was identified in colorectal cancers. PRRT4 has not been reported in any study yet. The information mentioned above adds credibility to the regulatory axes. The more information that is validated by experiments, the higher the reliability of the regulatory axis. In contrast, the higher the predictability of the axis, the greater the significance of further experimental confirmation. Therefore, the reliability of the OPCML axis, the FAT3 axis, the FXYD6 axis and the

PRRT4 axis decreases in that order, and their predictability increases in that order.

In this study, we selected the POU6F2-AS2/hsa-mir-137/OPCML axis with the highest reliability as an example. **Figure 7** shows a simplified diagram of the regulatory mechanism of this axis. The lncRNA POU6F2-AS2 in the axis was expressed at high levels, while hsa-mir-137 was expressed at low levels. Thus, the highly expressed lncRNA POU6F2-AS2, functioning as a ceRNA, sponged and downregulated the expression of hsa-mir-137, inhibited the expression of the target gene OPCML, and finally promoted the growth, proliferation, invasion, poor differentiation and poor prognosis of GC. We further predicted that the YBX1 protein might play an important role in this process. YBX1 (also called YB-1), a chromatin-binding protein, binds to single-stranded DNA (ssDNA) and pre-mRNA and mediates cell survival after DNA damage [27]. Numerous studies have shown that YBX1 mRNA and protein expression is significantly increased in GC and other cancers [28-30]. The increase in YBX1 protein levels is significantly associated with the migration process of GC [28]. The lncRNA POU6F2-AS2 targets and binds YBX1, and it is indispensable for the binding of YBX1 to chromatin [31]. In addition, YBX1 compensates for the repair function of POU6F2-AS2 in the DNA damage response to ionizing radiation (IR) treatment [31], which leads to treatment failure and undesirable outcomes. In 2016, Liu J et al. found that POU6F2-AS2, which is expressed at high levels in patients with squamous cell esophageal cancer, was significantly related to the high invasiveness of cancer tissues and resistance to radiotherapy [31]. POU6F2-AS2 knockout inhibited the locating and binding of YBX1 to damaged DNA, thereby increasing the amount of DNA damage in cancer cells and improving the radiotherapy sensitivity of cancer tissues [31]. Based on the evidence mentioned above, we speculated that the repair function of POU6F2-AS2 and YBX1 might explain why GC cells can proliferate in the presence of DNA damage from IR or immune elimination. Moreover, the miRNA hsa-mir-137 also directly or indirectly downregulates the expression of the YBX1 protein. In 2018, Chu PC et al. showed that highly expressed miR-137 inhibited YBX1 expression by targeting the 3'UTR of YBX1 [32]. In 2018, Johnson TG et al. performed cell-based experiments and observed that transfection of miR-137 analogs inhibited the growth, metastasis and invasion of cancer cells, and this process was related to the direct downregulation of YBX1 expression [33]. Based on the above-mentioned results, we infer that the downregulation of miR-137 expression, in addition to downregulating the expression of OPCML to promote GC cell proliferation and treatment resistance, might weaken the inhibition of YBX1 expression and thus increase the level of the YBX1 protein. The increased YBX1 level, together with the highly expressed POU6F2-AS2, suppresses DNA repair and promotes the survival of DNA-damaged cells. Similar to the mechanism by which the members of the POU6F2-AS2/hsa-mir-137/OPCML axis regulate each other in GC and participate in the oncogenesis and development of cancer, we hypothesize that the other three axes predicted in this study also play important roles in the progression and malignant biological processes of GC.

We conducted functional enrichment and pathway analyses of 204 mRNAs in the ceRNA network to further explore the mechanisms of the 204 mRNAs in the ceRNA network in GC. As shown in **Figure 4A**, the trans-synaptic signaling cluster was the most significant GO function cluster identified, which included 7 terms (trans-synaptic signaling, synaptic signaling, chemical synaptic transmission, anterograde trans-synaptic signaling, modulation of chemical synaptic transmission, regulation of trans-synaptic signaling, and regulation of membrane potential) (Supplementary Table 3). Among the 7 terms, regulation of membrane potential processes (GO: 0042391) has been reported to have an important function in GC [34]. The most significant KEGG cluster was the protein digestion and absorption cluster, which included 12 terms (protein digestion and absorption [ko04974], protein digestion and absorption [hsa04974], extracellular matrix, external encapsulating structure, collagen-containing extracellular matrix, extracellular matrix organization, extracellular structure organization, external encapsulating structure organization, collagen trimer, extracellular matrix structural constituent conferring tensile strength, extracellular matrix structural constituent, and structural molecule activity) (Supplementary Table 3). Among these 12 terms, 6 terms (protein diges-

tion and absorption [hsa04974], extracellular matrix, collagen-containing extracellular matrix, extracellular matrix organization, extracellular matrix structural constituent, and structural molecule activity) have been reported to play important roles in the function of mRNAs in GC [35-38], and 5 candidate prognostic biomarkers (SERPINE1, ADAMTS18, COL3A1, COL10A1, and COL21A1) were enriched in them. Notably, these five biomarkers were confirmed experimentally either in GC (the former four) or in head and neck cancer (the final one) (**Table 4**), indicating their potential function in the six signaling pathways and the reliability of our study. In addition, in the network of enriched terms (**Figure 4B** and **4C**), the largest subnetwork included 5 clusters (trans-synaptic signaling, post synapse, regulation of system process, inorganic molecular entity transmembrane transporter activity and regulation of ion transport) that were in close proximity and intertwined in space, suggesting that they might be functionally relevant to each other and play an important role in the progression and invasion process of gastric tumor cells together. Among these 5 clusters, FXYD6, a potential prognostic target, was enriched in the post synapse cluster, regulation of system process cluster and regulation of ion transport cluster (Supplementary Table 3). Thus, we speculate that the prognostic FXYD6 and POU6F2-AS2/hsa-mir-137/FXYD6 regulatory axis might affect the pathogenesis of GC by acting on the above three clusters. However, the specific mechanisms still need to be clarified in further studies.

As of February 28, 2022, 63 GC studies related to the ceRNA network have been retrieved from PubMed. Among the 63 articles, five were review articles, 38 were experimental studies (the majority of them did not construct a whole lncRNA (circRNA)/miRNA/mRNA ceRNA axis) and 20 were theoretical studies (among them, only 3 also proposed a complete DElncRNA (DEcircRNA)/DEmiRNA/DEmRNA axis). In 2020, Chen J et al. analyzed DElncRNAs, DEmiRNAs and immune-related DEmRNAs in GC derived from patient samples stored in GEO databases to construct an immune microenvironment-related ceRNA network and proposed two ceRNA regulatory axes (AC104389.28/miR-17-5/SMAD5 axis and LINC01133/miR-17-5p/PBLD axis) [39]. In the same year, Li JX et al. obtained DElncRNA, DEmiRNA and DEmRNA data using the patient samples of gastric tumor in TCGA, GEO and GEPIA (http://gepia.cancer-pku.cn/) databases to construct a prognosis-related ceRNA network and predicted four prognostic ceRNA axes (H19/miR-29a-3p/COL4A1 or COL1A2 or COL5A2 or COL3A1 axes) [40]. In 2021, Li Y et al. derived DEcircRNAs, DEmiRNAs and DEmRNAs in gastric cancer from the patient samples also stored in the GEO and TCGA databases to construct a prognosis-unrelated ceRNA network and further proposed 3 potential regulatory axes (hsa_circ_0058097/hsa_miR_145-5p/SERPINE1 axis, hsa_circ_0058097/hsa_miR_133a-3p/COL1A1 axis, and hsa_circ_0058097/hsa_miR_1-3p/MET axis) [41]. However, deep speculation or discussion of the underlying mechanisms of these axes are lacking in these three studies.

In the present study, (1) we thoroughly compared the abnormal expression of 43 candidate prognostic RNA targets (13 lncRNAs, 2 miRNAs, and 28 mRNAs) in GC from our calculation with those reported in the existing related literature to confirm the reliability and predictability of our study. (2) Enrichment analyses of 204 mRNAs in the ceRNA network revealed the importance of the trans-synaptic signaling cluster as well as the protein digestion and absorption cluster during the aggressive process of GC. (3) In addition to predicting four theoretical lncRNA/miRNA/mRNA axes based on the regulatory relationship of a prognosis-related ceRNA network, we also evaluated the possibility and stability of these axes through the existing experimental literature and further specifically clarified the regulatory mechanism and functional processes of the POU6F2-AS2/hsa-mir-137/OPCML axis. Although the regulatory mechanisms at the transcriptional level and the reliability of these four axes still require verification in future studies, further investigation of these axes in GC would help us understand their key roles in more comprehensive and multilevel ways, and it would facilitate a more precise diagnosis that enables earlier intervention and provides a better prognosis for patients with GC.

Conclusions

In summary, our study used bioinformatics methods to construct a ceRNA network for GC and identified 43 candidate biomarkers (13 lncRNAs, 2 miRNAs, and 28 mRNAs) that were

closely associated with the diagnosis and poor prognosis of patients with GC. Among them, two lncRNAs (LNC00469 and AC010145.1) and one mRNA (PRRT4) were novel biomarkers that were discovered for the first time in this study. In addition, based on the regulatory relationships in the ceRNA network, we established four lncRNA/miRNA/mRNA regulatory axes (POU6F2-AS/hsa-mir-137/OPCML, POU6F2-AS2/hsa-mir-137/FAT3, POU6F2-AS2/hsa-mir-137/FXYD6, and POU6F2-AS2/hsa-mir-137/PRRT4) from the 43 DERNA-os. The POU6F2-AS2/hsa-mir-137/OPCML axis containing YBX1 possessed the highest reliability. 204 mRNAs in the ceRNA network might affect the progression of GC through the trans-synaptic signaling cluster and the protein digestion and absorption cluster. In summary, we analyzed the changes in the expression of RNAs and their functions in GC from the perspective of the ceRNA network, including lncRNAs, miRNAs and mRNAs, and identified candidate biomarkers for clinical diagnosis, treatment, drug research, and prognosis. In addition, we identified four potential axes to help study the mechanisms underlying the carcinogenesis and progression of GC in the future.

Acknowledgements

This work was funded by the Key Discipline Construction Project of Guangdong Medical University [4SG21004G] and the Higher Education Reform Project of Guangdong Province [2019268]. We thank American Journal Experts (AJE) for their help in revising the English grammar.

Disclosure of conflict of interest

None.

Address correspondence to: Zunnan Huang, Guangdong Medical University, No. 1 Xincheng Road, Songshan Lake District, Dongguan 523808, Guangdong, China. Tel: +86-1392559-0670, E-mail: zn_huang@gdmu.edu.cn

References

[1] Sung H, Ferlay J, Siegel RL, Laversanne M, Soerjomataram I, Jemal A and Bray F. Global Cancer statistics 2020: Globocan estimates of incidence and mortality worldwide for 36 cancers in 185 countries. CA Cancer J Clin 2021; 71: 209-249.

[2] Cao W, Chen HD, Yu YW, Li N and Chen WQ. Changing profiles of cancer burden worldwide and in China: a secondary analysis of the global cancer statistics 2020. Chin Med J (Engl) 2021; 134: 783-791.

[3] Chen JG, Chen HZ, Zhu J, Yang YL, Zhang YH, Huang PX, Chen YS, Zhu CY, Yang LP, Shen K, Qiang FL and Wang GR. Cancer survival in patients from a hospital-based cancer registry, China. J Cancer 2018; 9: 851-860.

[4] Carninci P, Kasukawa T, Katayama S, Gough J, Frith MC, Maeda N, Oyama R, Ravasi T, Lenhard B, Wells C, Kodzius R, Shimokawa K, Bajic VB, Brenner SE, Batalov S, Forrest AR, Zavolan M, Davis MJ, Wilming LG, Aidinis V, Allen JE, Ambesi-Impiombato A, Apweiler R, Aturaliya RN, Bailey TL, Bansal M, Baxter L, Beisel KW, Bersano T, Bono H, Chalk AM, Chiu KP, Choudhary V, Christoffels A, Clutterbuck DR, Crowe ML, Dalla E, Dalrymple BP, de Bono B, Della Gatta G, di Bernardo D, Down T, Engstrom P, Fagiolini M, Faulkner G, Fletcher CF, Fukushima T, Furuno M, Futaki S, Gariboldi M, Georgii-Hemming P, Gingeras TR, Gojobori T, Green RE, Gustincich S, Harbers M, Hayashi Y, Hensch TK, Hirokawa N, Hill D, Huminiecki L, Iacono M, Ikeo K, Iwama A, Ishikawa T, Jakt M, Kanapin A, Katoh M, Kawasawa Y, Kelso J, Kitamura H, Kitano H, Kollias G, Krishnan SP, Kruger A, Kummerfeld SK, Kurochkin IV, Lareau LF, Lazarevic D, Lipovich L, Liu J, Liuni S, McWilliam S, Madan Babu M, Madera M, Marchionni L, Matsuda H, Matsuzawa S, Miki H, Mignone F, Miyake S, Morris K, Mottagui-Tabar S, Mulder N, Nakano N, Nakauchi H, Ng P, Nilsson R, Nishiguchi S, Nishikawa S, Nori F, Ohara O, Okazaki Y, Orlando V, Pang KC, Pavan WJ, Pavesi G, Pesole G, Petrovsky N, Piazza S, Reed J, Reid JF, Ring BZ, Ringwald M, Rost B, Ruan Y, Salzberg SL, Sandelin A, Schneider C, Schönbach C, Sekiguchi K, Semple CA, Seno S, Sessa L, Sheng Y, Shibata Y, Shimada H, Shimada K, Silva D, Sinclair B, Sperling S, Stupka E, Sugiura K, Sultana R, Takenaka Y, Taki K, Tammoja K, Tan SL, Tang S, Taylor MS, Tegner J, Teichmann SA, Ueda HR, van Nimwegen E, Verardo R, Wei CL, Yagi K, Yamanishi H, Zabarovsky E, Zhu S, Zimmer A, Hide W, Bult C, Grimmond SM, Teasdale RD, Liu ET, Brusic V, Quackenbush J, Wahlestedt C, Mattick JS, Hume DA, Kai C, Sasaki D, Tomaru Y, Fukuda S, Kanamori-Katayama M, Suzuki M, Aoki J, Arakawa T, Iida J, Imamura K, Itoh M, Kato T, Kawaji H, Kawagashira N, Kawashima T, Kojima M, Kondo S, Konno H, Nakano K, Ninomiya N, Nishio T, Okada M, Plessy C, Shibata K, Shiraki T, Suzuki S, Tagami M, Waki K, Watahiki A, Okamura-Oho Y, Suzuki H, Kawai J and Hayashizaki Y. The transcriptional landscape of the mammalian genome. Science 2005; 309: 1559-1563.

[5] Djebali S, Davis CA, Merkel A, Dobin A, Lassmann T, Mortazavi A, Tanzer A, Lagarde J, Lin W, Schlesinger F, Xue C, Marinov GK, Khatun J, Williams BA, Zaleski C, Rozowsky J, Röder M, Kokocinski F, Abdelhamid RF, Alioto T, Antoshechkin I, Baer MT, Bar NS, Batut P, Bell K, Bell I, Chakrabortty S, Chen X, Chrast J, Curado J, Derrien T, Drenkow J, Dumais E, Dumais J, Duttagupta R, Falconnet E, Fastuca M, Fejes-Toth K, Ferreira P, Foissac S, Fullwood MJ, Gao H, Gonzalez D, Gordon A, Gunawardena H, Howald C, Jha S, Johnson R, Kapranov P, King B, Kingswood C, Luo OJ, Park E, Persaud K, Preall JB, Ribeca P, Risk B, Robyr D, Sammeth M, Schaffer L, See LH, Shahab A, Skancke J, Suzuki AM, Takahashi H, Tilgner H, Trout D, Walters N, Wang H, Wrobel J, Yu Y, Ruan X, Hayashizaki Y, Harrow J, Gerstein M, Hubbard T, Reymond A, Antonarakis SE, Hannon G, Giddings MC, Ruan Y, Wold B, Carninci P, Guigó R and Gingeras TR. Landscape of transcription in human cells. Nature 2012; 489: 101-108.

[6] Zhang M, Wu WB, Wang ZW and Wang XH. lncRNA NEAT1 is closely related with progression of breast cancer via promoting proliferation and EMT. Eur Rev Med Pharmacol Sci 2017; 21: 1020-1026.

[7] Su J, Liang H, Yao W, Wang N, Zhang S, Yan X, Feng H, Pang W, Wang Y, Wang X, Fu Z, Liu Y, Zhao C, Zhang J, Zhang CY, Zen K, Chen X and Wang Y. MiR-143 and MiR-145 regulate IGF1R to suppress cell proliferation in colorectal cancer. PLoS One 2014; 9: e114420.

[8] Salmena L, Poliseno L, Tay Y, Kats L and Pandolfi PP. A ceRNA hypothesis: the rosetta stone of a hidden RNA language? Cell 2011; 146: 353-358.

[9] Tay Y, Rinn J and Pandolfi PP. The multilayered complexity of ceRNA crosstalk and competition. Nature 2014; 505: 344-352.

[10] Lu R, Zhao G, Yang Y, Jiang Z, Cai J, Zhang Z and Hu H. Long noncoding RNA HOTAIRM1 inhibits cell progression by regulating miR-17-5p/PTEN axis in gastric cancer. J Cell Biochem 2019; 120: 4952-4965.

[11] Zhang Y, Yuan Y, Zhang Y, Cheng L, Zhou X and Chen K. SNHG7 accelerates cell migration and invasion through regulating miR-34a-Snail-EMT axis in gastric cancer. Cell Cycle 2020; 19: 142-152.

[12] Jeggari A, Marks DS and Larsson E. miRcode: a map of putative microRNA target sites in the long non-coding transcriptome. Bioinformatics 2012; 28: 2062-2063.

[13] Chen Y and Wang X. miRDB: an online database for prediction of functional microRNA targets. Nucleic Acids Res 2020; 48: D127-d131.

[14] Agarwal V, Bell GW, Nam JW and Bartel DP. Predicting effective microRNA target sites in mammalian mRNAs. Elife 2015; 4: e05005.

[15] Reczko M, Maragkakis M, Alexiou P, Grosse I and Hatzigeorgiou AG. Functional microRNA targets in protein coding sequences. Bioinformatics 2012; 28: 771-776.

[16] Paraskevopoulou MD, Georgakilas G, Kostoulas N, Vlachos IS, Vergoulis T, Reczko M, Filippidis C, Dalamagas T and Hatzigeorgiou AG. DIANA-microT web server v5.0: service integration into miRNA functional analysis workflows. Nucleic Acids Res 2013; 41: W169-173.

[17] Shannon P, Markiel A, Ozier O, Baliga NS, Wang JT, Ramage D, Amin N, Schwikowski B and Ideker T. Cytoscape: a software environment for integrated models of biomolecular interaction networks. Genome Res 2003; 13: 2498-2504.

[18] Zhou Y, Zhou B, Pache L, Chang M, Khodabakhshi AH, Tanaseichuk O, Benner C and Chanda SK. Metascape provides a biologist-oriented resource for the analysis of systems-level datasets. Nat Commun 2019; 10: 1523.

[19] Kaplan EL and Meier P. Nonparametric estimation from incomplete observations. Journal of the American Statistical Association 1958; 53: 457-481.

[20] Du W, Wang S, Zhou Q, Li X, Chu J, Chang Z, Tao Q, Ng EK, Fang J, Sung JJ and Yu J. ADAMTS9 is a functional tumor suppressor through inhibiting AKT/mTOR pathway and associated with poor survival in gastric cancer. Oncogene 2013; 32: 3319-3328.

[21] Hu X, Li Y, Kong D, Hu L, Liu D and Wu J. Long noncoding RNA CASC9 promotes LIN7A expression via miR-758-3p to facilitate the malignancy of ovarian cancer. J Cell Physiol 2019; 234: 10800-10808.

[22] Wu Y, Wang A, Zhu B, Huang J, Lu E, Xu H, Xia W, Dong G, Jiang F and Xu L. KIF18B promotes tumor progression through activating the Wnt/β-catenin pathway in cervical cancer. Onco Targets Ther 2018; 11: 1707-1720.

[23] Mattick JS and Makunin IV. Non-coding RNA. Hum Mol Genet 2006; 15 Spec No 1: R17-29.

[24] Chan JJ and Tay Y. Noncoding RNA: RNA regulatory networks in cancer. Int J Mol Sci 2018; 19: 1310.

[25] Brown BD, Gentner B, Cantore A, Colleoni S, Amendola M, Zingale A, Baccarini A, Lazzari G, Galli C and Naldini L. Endogenous microRNA can be broadly exploited to regulate transgene expression according to tissue, lineage and differentiation state. Nat Biotechnol 2007; 25: 1457-1467.

[26] Arvey A, Larsson E, Sander C, Leslie CS and Marks DS. Target mRNA abundance dilutes microRNA and siRNA activity. Mol Syst Biol 2010; 6: 363.

[27] Kim ER, Selyutina AA, Buldakov IA, Evdokimova V, Ovchinnikov LP and Sorokin AV. The proteolytic YB-1 fragment interacts with DNA re-

pair machinery and enhances survival during DNA damaging stress. Cell Cycle 2013; 12: 3791-3803.
[28] Guo TT, Yu YN, Yip GW, Matsumoto K and Bay BH. Silencing the YB-1 gene inhibits cell migration in gastric cancer in vitro. Anat Rec (Hoboken) 2013; 296: 891-898.
[29] Su W, Feng S, Chen X, Yang X, Mao R, Guo C, Wang Z, Thomas DG, Lin J, Reddy RM, Orringer MB, Chang AC, Yang Z, Beer DG and Chen G. Silencing of long noncoding RNA MIR22HG triggers cell survival/death signaling via oncogenes YBX1, MET, and p21 in lung cancer. Cancer Res 2018; 78: 3207-3219.
[30] Lim JP, Shyamasundar S, Gunaratne J, Scully OJ, Matsumoto K and Bay BH. YBX1 gene silencing inhibits migratory and invasive potential via CORO1C in breast cancer in vitro. BMC Cancer 2017; 17: 201.
[31] Liu J, Sun X, Zhu H, Qin Q, Yang X and Sun X. Long noncoding RNA POU6F2-AS2 is associated with oesophageal squamous cell carcinoma. J Biochem 2016; 160: 195-204.
[32] Chu PC, Lin PC, Wu HY, Lin KT, Wu C, Bekaii-Saab T, Lin YJ, Lee CT, Lee JC and Chen CS. Mutant KRAS promotes liver metastasis of colorectal cancer, in part, by upregulating the MEK-Sp1-DNMT1-miR-137-YB-1-IGF-IR signaling pathway. Oncogene 2018; 37: 3440-3455.
[33] Johnson TG, Schelch K, Cheng YY, Williams M, Sarun KH, Kirschner MB, Kao S, Linton A, Klebe S, McCaughan BC, Lin RCY, Pirker C, Berger W, Lasham A, van Zandwijk N and Reid G. Dysregulated expression of the microRNA miR-137 and its target YBX1 contribute to the invasive characteristics of malignant pleural mesothelioma. J Thorac Oncol 2018; 13: 258-272.
[34] Wang Y and Zhang J. Identification of differential expression lncRNAs in gastric cancer using transcriptome sequencing and bioinformatics analyses. Mol Med Rep 2018; 17: 8189-8195.
[35] Hu Y, Hu Z, Ding H, Li Y, Zhao X, Shao M and Pan Y. Identification of key biomarkers and potential signaling pathway associated with poor progression of gastric cancer. Transl Cancer Res 2020; 9: 5459-5472.
[36] Chen W, Zhang W, Wu R, Cai Y, Xue X and Cheng J. Identification of biomarkers associated with histological grade and prognosis of gastric cancer by co-expression network analysis. Oncol Lett 2019; 18: 5499-5507.
[37] Liang L, Zhu JH, Chen G, Qin XG and Chen JQ. Prognostic values for the mRNA expression of the ADAMTS family of genes in gastric cancer. J Oncol 2020; 2020: 9431560.
[38] Zhou W, Ouyang J, Li J, Liu F, An T, Cheng L, Kuo ZC, Zhang C and He Y. MRPS17 promotes invasion and metastasis through PI3K/AKT signal pathway and could be potential prognostic marker for gastric cancer. J Cancer 2021; 12: 4849-4861.
[39] Chen J, Chen JG, Sun B, Wu JH and Du CY. Integrative analysis of immune microenvironment-related CeRNA regulatory axis in gastric cancer. Math Biosci Eng 2020; 17: 3953-3971.
[40] Li J, Wang X, Wang Y and Yang Q. H19 promotes the gastric carcinogenesis by sponging miR-29a-3p: evidence from lncRNA-miRNA-mRNA network analysis. Epigenomics 2020; 12: 989-1002.
[41] Li Y, Li R, Wang X, Yuan Y and Zhang Y. A robust circular RNA-associated three-gene prognostic signature for patients with gastric cancer. Biomed Res Int 2021; 2021: 6633289.
[42] Teng F, Zhang JX, Chen Y, Shen XD, Su C, Guo YJ, Wang PH, Shi CC, Lei M, Cao YO and Liu SQ. LncRNA NKX2-1-AS1 promotes tumor progression and angiogenesis via upregulation of SERPINE1 expression and activation of the VEGFR-2 signaling pathway in gastric cancer. Mol Oncol 2021; 15: 1234-1255.
[43] Feng L, Li J, Li F, Li H, Bei S, Zhang X and Yang Z. Long noncoding RNA VCAN-AS1 contributes to the progression of gastric cancer via regulating p53 expression. J Cell Physiol 2020; 235: 4388-4398.
[44] Huang J, Chen YX and Zhang B. IGF2-AS affects the prognosis and metastasis of gastric adenocarcinoma via acting as a ceRNA of miR-503 to regulate SHOX2. Gastric Cancer 2020; 23: 23-38.
[45] Shan Y, Ying R, Jia Z, Kong W, Wu Y, Zheng S and Jin H. LINC00052 promotes gastric cancer cell proliferation and metastasis via activating the Wnt/β-Catenin signaling pathway. Oncol Res 2017; 25: 1589-1599.
[46] Liao Y, Cao W, Zhang K, Zhou Y, Xu X, Zhao X, Yang X, Wang J, Zhao S, Zhang S, Yang L, Liu D, Tian Y and Wu W. Bioinformatic and integrated analysis identifies an lncRNA-miRNA-mRNA interaction mechanism in gastric adenocarcinoma. Genes Genomics 2021; 43: 613-622.
[47] Wang F, Tang C, Xu D, Tang Y, Jiang Y, Gao X and Xu J. LncRNA ADAMTS9-AS2 suppresses the proliferation of gastric cancer cells and the tumorigenicity of cancer stem cells through regulating SPOP. J Cell Mol Med 2020; 24: 4830-4838.
[48] Wan J, Jiang S, Jiang Y, Ma W, Wang X, He Z, Wang X and Cui R. Data mining and expression analysis of differential lncRNA ADAMTS9-AS1 in prostate cancer. Front Genet 2020; 10: 1377.
[49] Liang Y, Zhang C and Dai DQ. Identification of DNA methylation-regulated differentially-expressed genes and related pathways using Illumina 450K BeadChip and bioinformatic

analysis in gastric cancer. Pathol Res Pract 2019; 215: 152570.
[50] Wu L, Chen J, Ding C, Wei S, Zhu Y, Yang W, Zhang X, Wei X and Han D. MicroRNA-137 Contributes to dampened tumorigenesis in human gastric cancer by targeting AKT2. PLoS one 2015; 10: e0130124.
[51] Deng J, Lei W, Xiang X, Zhang L, Lei J, Gong Y, Song M, Wang Y, Fang Z, Yu F, Feng M, Sun Z, Chen J, Zhan Z and Xiong J. Cullin 4A (CUL4A), a direct target of miR-9 and miR-137, promotes gastric cancer proliferation and invasion by regulating the Hippo signaling pathway. Oncotarget 2016; 7: 10037-10050.
[52] Lei C, Du F, Sun L, Li T, Li T, Min Y, Nie A, Wang X, Geng L, Lu Y, Zhao X, Shi Y and Fan D. miR-143 and miR-145 inhibit gastric cancer cell migration and metastasis by suppressing MYO6. Cell Death Dis 2017; 8: e3101.
[53] Zeng JF, Ma XQ, Wang LP and Wang W. MicroRNA-145 exerts tumor-suppressive and chemoresistance lowering effects by targeting CD44 in gastric cancer. World J Gastroenterol 2017; 23: 2337-2345.
[54] Yang JD, Ma L and Zhu Z. SERPINE1 as a cancer-promoting gene in gastric adenocarcinoma: facilitates tumour cell proliferation, migration, and invasion by regulating EMT. J Chemother 2019; 31: 408-418.
[55] Kilic MO, Aynekin B, Kara A, Icen D and Demircan K. Differentially regulated ADAMTS1, 8, and 18 in gastric adenocarcinoma. Bratisl Lek Listy 2017; 118: 71-76.
[56] Chen ZL, Qin L, Peng XB, Hu Y and Liu B. INHBA gene silencing inhibits gastric cancer cell migration and invasion by impeding activation of the TGF-β signaling pathway. J Cell Physiol 2019; 234: 18065-18074.
[57] Zhang C, Li Z, Xu L, Che X, Wen T, Fan Y, Li C, Wang S, Cheng Y, Wang X, Qu X and Liu Y. CXCL9/10/11, a regulator of PD-L1 expression in gastric cancer. BMC Cancer 2018; 18: 462.
[58] Li C, Zhang J, Wu H, Li L, Yang C, Song S, Peng P, Shao M, Zhang M, Zhao J, Zhao R, Wu W, Ruan Y, Wang L and Gu J. Lectin-like oxidized low-density lipoprotein receptor-1 facilitates metastasis of gastric cancer through driving epithelial-mesenchymal transition and PI3K/Akt/GSK3β activation. Sci Rep 2017; 7: 45275.
[59] He YX, Song XH, Zhao ZY and Zhao H. HOXA13 upregulation in gastric cancer is associated with enhanced cancer cell invasion and epithelial-to-mesenchymal transition. Eur Rev Med Pharmacol Sci 2017; 21: 258-265.
[60] Chen Z, Soutto M, Rahman B, Fazili MW, Peng D, Piazuelo MB, Chen H, Washington MK, Shyr Y and El-Rifai W. Integrated expression analysis identifies transcription networks in mouse and human gastric neoplasia. Genes Chromosomes Cancer 2017; 56: 535-547.
[61] Wang J, Zhang Y, Dou Z, Jiang H, Wang Y, Gao X and Xin X. Knockdown of STIL suppresses the progression of gastric cancer by down-regulating the IGF-1/PI3K/AKT pathway. J Cell Mol Med 2019; 23: 5566-5575.
[62] Li T, Huang H, Shi G, Zhao L, Li T, Zhang Z, Liu R, Hu Y, Liu H, Yu J and Li G. TGF-β1-SOX9 axis-inducible COL10A1 promotes invasion and metastasis in gastric cancer via epithelial-to-mesenchymal transition. Cell Death Dis 2018; 9: 849.
[63] Ke H, Wu S, Zhang Y and Zhang G. miR-139-3p/Kinesin family member 18B axis suppresses malignant progression of gastric cancer. Bioengineered 2022; 13: 4528-4536.
[64] Zhang M, Zhang C, Du W, Yang X and Chen Z. ATAD2 is overexpressed in gastric cancer and serves as an independent poor prognostic biomarker. Clin Transl Oncol 2016; 18: 776-781.
[65] Hong SA, Yoo SH, Lee HH, Sun S, Won HS, Kim O and Ko YH. Prognostic value of Dickkopf-1 and ß-catenin expression in advanced gastric cancer. BMC Cancer 2018; 18: 506.
[66] Luo T, Zhao J, Lu Z, Bi J, Pang T, Cui H, Yang B, Li W, Wang Y, Wu S and Xue X. Characterization of long non-coding RNAs and MEF2C-AS1 identified as a novel biomarker in diffuse gastric cancer. Transl Oncol 2018; 11: 1080-1089.
[67] Kim SK, Jang HR, Kim JH, Noh SM, Song KS, Kim MR, Kim SY, Yeom YI, Kim NS, Yoo HS and Kim YS. The epigenetic silencing of LIMS2 in gastric cancer and its inhibitory effect on cell migration. Biochem Biophys Res Commun 2006; 349: 1032-1040.
[68] Xing X, Cai W, Ma S, Wang Y, Shi H, Li M, Jiao J, Yang Y, Liu L, Zhang X and Chen M. Down-regulated expression of OPCML predicts an unfavorable prognosis and promotes disease progression in human gastric cancer. BMC Cancer 2017; 17: 268.
[69] Chun SH, Kim EY, Yoon JS, Won HS, Yim K, Hwang HW, Hong SA, Lee M, Lee SL, Kim SS, Sun S and Ko YH. Prognostic value of noggin protein expression in patients with resected gastric cancer. BMC Cancer 2021; 21: 558.
[70] Miao Y, Li Q, Sun G, Wang L, Zhang D, Xu H and Xu Z. MiR-5683 suppresses glycolysis and proliferation through targeting pyruvate dehydrogenase kinase 4 in gastric cancer. Cancer Med 2020; 9: 7231-7243.
[71] Liu NQ, Huurne MT, Nguyen LN, Peng T, Wang SY, Studd JB, Joshi O, Ongen H, Bramsen JB, Yan J, Andersen CL, Taipale J, Dermitzakis ET, Houlston RS, Hubner NC and Stunnenberg HG. The non-coding variant rs1800734 enhances DCLK3 expression through long-range interac-

tion and promotes colorectal cancer progression. Nat Commun 2017; 8: 14418.
[72] Long PM, Moffett JR, Namboodiri AAM, Viapiano MS, Lawler SE and Jaworski DM. N-acetylaspartate (NAA) and N-acetylaspartylglutamate (NAAG) promote growth and inhibit differentiation of glioma stem-like cells. J Biol Chem 2013; 288: 26188-26200.
[73] Misawa K, Kanazawa T, Imai A, Endo S, Mochizuki D, Fukushima H, Misawa Y and Mineta H. Prognostic value of type XXII and XXIV collagen mRNA expression in head and neck cancer patients. Mol Clin Oncol 2014; 2: 285-291.
[74] Luo W, Liu Q, Chen X, Liu H, Quan B, Lu J, Zhang K and Wang X. FXYD6 regulates chemosensitivity by mediating the expression of Na+/K+-ATPase α1 and affecting cell autophagy and apoptosis in colorectal cancer. Biomed Res Int 2021; 2021: 9986376.
[75] Fouad EM, Harb OA, Amin SR, Farargy OME, Habib FM and Gertallah LM. The Expression of FOXE-1 and STIP-1 in Papillary Thyroid carcinoma and their relationship with patient prognosis. Iran J Pathol 2018; 13: 256-271.
[76] Morelli MB, Amantini C, Nabissi M, Liberati S, Cardinali C, Farfariello V, Tomassoni D, Quaglia W, Piergentili A, Bonifazi A, Bello FD, Santoni M, Mammana G, Servi L, Filosa A, Gismondi A and Santoni G. Cross-talk between alpha1D-adrenoceptors and transient receptor potential vanilloid type 1 triggers prostate cancer cell proliferation. BMC Cancer 2014; 14: 921.
[77] Wang CJ, Zhang ZZ, Xu J, Wang M, Zhao WY, Tu L, Zhuang C, Liu Q, Shen YY, Cao H and Zhang ZG. SLITRK3 expression correlation to gastrointestinal stromal tumor risk rating and prognosis. World J Gastroenterol 2015; 21: 8398-8407.
[78] Cheon H, Xing JC, Moosic KB, Ung J, Chan V, Chung DS, Toro MF, Elghawy O, Wang JS, Hamele CE, Hardison RC, Olson TL, Tan SF, Feith D, Aakrosh R and Loughran T. Genomic landscape of TCR alpha-beta and TCR gamma-delta T-large granular lymphocyte leukemia. Blood 2022; blood.2021013164.
[79] Wang W, Wang S, Chu X, Liu H and Xiang M. Predicting the lung squamous cell carcinoma diagnosis and prognosis markers by unique DNA methylation and gene expression profiles. J Comput Biol 2020; 27: 1041-1054.
[80] Matsusaka K, Kaneda A, Nagae G, Ushiku T, Kikuchi Y, Hino R, Uozaki H, Seto Y, Takada K, Aburatani H and Fukayama M. Classification of Epstein-Barr virus-positive gastric cancers by definition of DNA methylation epigenotypes. Cancer Res 2011; 71: 7187-7197.
[81] Li ZM, Zhang HY, Wang YX and Wang WB. MicroRNA-137 is downregulated in human osteosarcoma and regulates cell proliferation and migration through targeting FXYD6. J Drug Target 2016; 24: 102-110.

Supplementary Table 1. The DElncRNA-DEmiRNA pairs in ceRNA network

lncRNA	miRNA
POU6F2-AS2	**hsa-mir-137**, hsa-mir-383
ADAMTS9-AS2	hsa-mir-372, hsa-mir-373, **hsa-mir-137**, **hsa-mir-145**, hsa-mir-184, hsa-mir-205, hsa-mir-122
C8orf31	hsa-mir-372, hsa-mir-373, hsa-mir-122
HOTTIP	hsa-mir-372, hsa-mir-373, **hsa-mir-137**, hsa-mir-519d, hsa-mir-184, hsa-mir-205
DLX6-AS1	hsa-mir-372, hsa-mir-373, **hsa-mir-145**, hsa-mir-519d, hsa-mir-122, hsa-mir-383
LINC00184	hsa-mir-372, hsa-mir-373, **hsa-mir-145**, hsa-mir-519d, hsa-mir-205
LINC00330	hsa-mir-372, hsa-mir-373, **hsa-mir-145**, hsa-mir-519d, hsa-mir-205, hsa-mir-122, hsa-mir-383
LINC00534	hsa-mir-372, hsa-mir-373, hsa-mir-205
AL356133.2	hsa-mir-372, hsa-mir-373, hsa-mir-383
C17orf77	hsa-mir-372, hsa-mir-373, hsa-mir-519d
AP002478.1	hsa-mir-372, hsa-mir-373, hsa-mir-519d, hsa-mir-184, hsa-mir-205, hsa-mir-508, hsa-mir-122
ARHGEF26-AS1	hsa-mir-372, hsa-mir-373, hsa-mir-519d, hsa-mir-205, hsa-mir-508
LINC00221	hsa-mir-372, hsa-mir-373, hsa-mir-519d, hsa-mir-508
DSCAM-AS1	**hsa-mir-137**, hsa-mir-122
DSCR8	**hsa-mir-137**, hsa-mir-205, hsa-mir-122
LINC00326	**hsa-mir-137**, hsa-mir-205, hsa-mir-383
ADAMTS9-AS1	**hsa-mir-145**
MIR205HG	**hsa-mir-145**, hsa-mir-205, hsa-mir-122, hsa-mir-383
DIRC3	**hsa-mir-145**, hsa-mir-205, hsa-mir-508
PART1	**hsa-mir-145**, hsa-mir-205, hsa-mir-508, hsa-mir-122
HCG22	**hsa-mir-145**, hsa-mir-508, hsa-mir-122, hsa-mir-383
DSCR4	**hsa-mir-145**, hsa-mir-508, hsa-mir-383
NKX2-1-AS1	**hsa-mir-145**, hsa-mir-519d
LINC00052	**hsa-mir-145**, hsa-mir-519d
PLCH1-AS2	hsa-mir-122
LINC00355	hsa-mir-122
AC090398.1	hsa-mir-122
AC026320.1	hsa-mir-122
AC018781.1	hsa-mir-122
AC010145.1	hsa-mir-122, hsa-mir-383
OSTN-AS1	**hsa-mir-137**
AC138761.1	**hsa-mir-137**
AC034229.1	**hsa-mir-137**
FRMD6-AS2	hsa-mir-184
BOK-AS1	hsa-mir-184
AC110619.1	hsa-mir-184, hsa-mir-122
UCA1	hsa-mir-184, hsa-mir-122, hsa-mir-383
LINC00524	hsa-mir-205
IL20RB-AS1	hsa-mir-205
ERVMER61-1	hsa-mir-205
ADARB2-AS1	hsa-mir-205
AC006449.1	hsa-mir-205
AC110491.1	hsa-mir-205, hsa-mir-508
C15orf54	hsa-mir-372, hsa-mir-373
LINC00393	hsa-mir-372, hsa-mir-373
CECR3	hsa-mir-372, hsa-mir-373
AC061975.6	hsa-mir-372, hsa-mir-373

AC011374.1	hsa-mir-372, hsa-mir-373
C7orf69	hsa-mir-383
AL391832.1	hsa-mir-383
AL357153.1	hsa-mir-383
LINC00469	hsa-mir-508
LINC00114	hsa-mir-508
DSCR4-IT1	hsa-mir-508
LINC00523	hsa-mir-508, hsa-mir-122
LINC00112	hsa-mir-508, hsa-mir-122
LINC00454	hsa-mir-519d
LINC00365	hsa-mir-519d
LINC00200	hsa-mir-519d
HOTAIR	hsa-mir-519d
H19	hsa-mir-519d
DAOA-AS1	hsa-mir-519d
AL391152.1	hsa-mir-519d
AC061975.6	hsa-mir-519d
AC002511.1	hsa-mir-519d
IGF2-AS	hsa-mir-519d, hsa-mir-122
LINC00410	hsa-mir-519d, hsa-mir-205, hsa-mir-122
AC092422.1	hsa-mir-519d, hsa-mir-383

Note: the RNAs marked in bold were prognostic significantly in gastric cancer.

Supplementary Table 2. The DEmiRNA-DEmRNA pairs in ceRNA network

miRNA	Gene (mRNA)
hsa-mir-122	NOS1, SLC25A34, IL1RN, SLC13A5
hsa-mir-137	**FXYD6**, LBX1, KCNA1, AQP2, HLF, ENHO, PROX1, GPR158, ATP2B2, EPHA7, NEGR1, RNF150, NRXN1, E2F7, SLC5A7, SLC17A6, HOXD10, **OPCML**, GRID2, APLN, EN2, SCRT1, RYR3, PTN, FGL2, HTR2C, CADM2, **PRRT4**, ESRRG, LRRC10B, SGCG, DCDC2, CTNNA3, ACTN2, CA7, FNDC5, SHISA9, **FAT3**, NEUROD4, LGI3, KLF15, KCNB1
hsa-mir-145	FOXE1, MAPK4, DLX6, RBM20
hsa-mir-184	HAND2
hsa-mir-205	TP53AIP1, EN1, EPGN, GPR158, LIN28B, NEGR1, **PCDHA12**, GPM6A, ASB4, NOX3, GABRP, EN2, SULF1, PTCHD1, KCNJ16, CKB, CAPN14, PAX9, CLDN2, STRIP2, ESRRG, **PCDHA11**, SH3GL3, AFM, PSG1, GJB7, **COL3A1**, ABCG2, WDR72, TRIM71, FAM133A, LMO3, HMGCLL1, CAP2, NRCAM, CENPF, **HOXA13**, **LIMS2**, BAMBI, APOBEC2, KCNJ13, PROX1, EPHA7, RNF150, **PDK4**, **ZNF365**, VWC2, SPHKAP, GRIA4, RYR3, COL22A1, SLC28A3, FABP7, CADM2, **COL21A1**, CXCL11, C11orf86, **ASPA**, CLVS2, PMCH, **RBPMS2**, SLC6A14, CTNNA3, BMPER, **INHBA**, SORBS1, SLC35D3, **CXCL9**, **DKK1**, DTL, MEST, NPY2R, **COL10A1**, PAH
hsa-mir-372	COL1A1, GPR158, NEGR1, **PCDHA12**, MME, NR4A3, E2F7, GPM6A, CDCA2, KIF26B, CACNA1E, STRIP2, **PCDHA11**, NR2E1, TMEM100, ABCG2, FOXL2, ISM2, LMO3, KCNB1, C2CD4A, KCNA1, BAMBI, HLF, ECT2, MEX3A, OLFM3, DRD1, FGL2, **ADAMTS18**, CADM2, ZNF716, LEFTY1, ADRB2, DCDC2, **ATAD2**, **NECAB1**, PPP1R3C
hsa-mir-373	GPR158, **OLR1**, **PCDHA12**, NR4A3, E2F7, GPM6A, VIP, PGR, CLEC5A, MAB21L1, KIF26B, CACNA1E, PON1, **KIF18B**, RIPPLY3, STRIP2, **PCDHA11**, NR2E1, TMEM100, ABCG2, FOXL2, ISM2, LMO3, KCNB1, ZIC2, BAMBI, HLF, ADAMTS2, **ADRA1D**, ECT2, **ZNF365**, MEX3A, LRP2, FGL2, **ADAMTS18**, CADM2, ANGPTL7, LEFTY1, RGS21, CLVS2, DCDC2, CTNNA3, **ATAD2**, **FAT3**, CSN1S1, SIGLEC11, PMEPA1
hsa-mir-383	CCNE1, NEGR1, NR4A3, MALL, LCE1E, MAGEA12, OTC, CACNA1E, **KIF18B**, TMEM154, MAGEA2B, MAGEA6, NXPH1, MAGEA2, HLF, HOXD13, MAGEA3, MTUS2, SORCS1, LIN28B
hsa-mir-508	LIN28B, ASCL2, NR4A3, KCNG3, EXO1, C17orf78, CRISP3, **STIL**, SLC39A2, LMO3, CYP3A4, GRM8, SIX3, DLX6, EMP1, SORCS1, SALL4, HJURP, FLG, GRIA2
hsa-mir-519d	BTG2, ATP2B2, **PCDHA12**, NR4A3, SMOC2, **SLITRK3**, IL36RN, KIF26B, SLC15A5, SYT10, FAT2, STRIP2, **PCDHA11**, RFX8, TMEM100, TBX4, FOXL2, ISM2, TRIM71, SLC2A4, LMO3, KCNB1, IGF2BP1, C2CD4A, **DCLK3**, CNN1, BAMBI, HLF, PROX1, EPHA7, MSR1, PSD, TNFSF11, GRID2, ANKRD30A, OLFM3, SLC28A3, SLC6A4, CADM2, MAGEA9, CLVS2, DCDC2, HMGA2, ATP1A2, **ATAD2**, CHRM2, **SERPINE1**, CXCL6

Note: the RNAs marked in bold were prognostic significantly in gastric cancer.

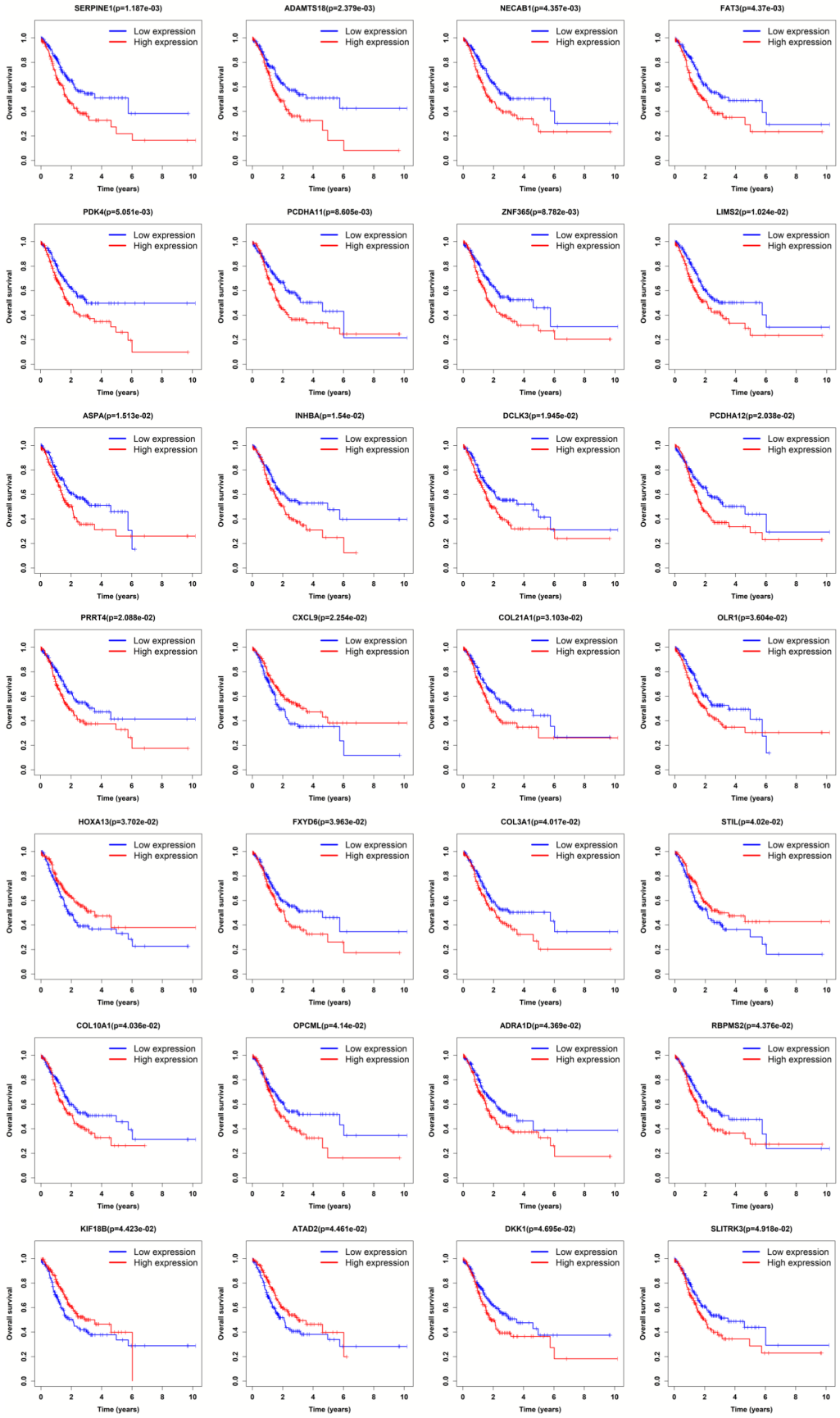

Supplementary Figure 1. Survival curves of 28 mRNAs in the ceRNA network.